From actinides to superheavy nuclei: benchmarking theory and addressing theoretical uncertainties

Anatoli Afanasjev

Mississippi State University

1. Introduction
2. Actinides as a testing ground
   - single-particle degrees of freedom
   - rotational excitations
   - fission barriers
3. Extrapolation to superheavy nuclei
   - shell structure reanalysed
   - deformation properties
   - fission barriers
4. Some thoughts on improving single-particle properties: (quasiparticle-vibration coupling versus tensor force)
5. Conclusions

Covariant density functional theory (CDFT)

The nucleons interact via the exchange of effective mesons →
→ **effective Lagrangian**

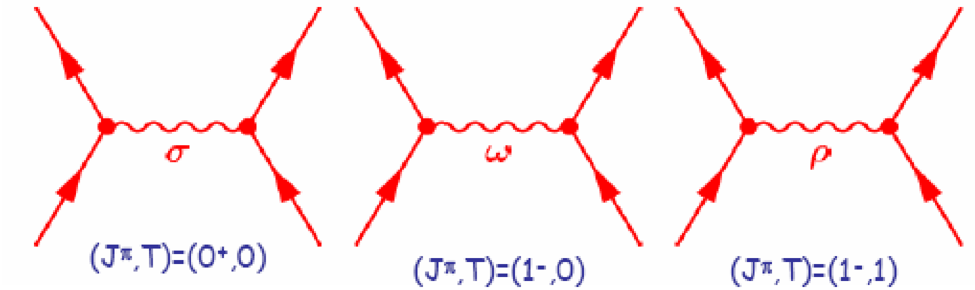

Long-range attractive scalar field

Short-range repulsive vector field

Isovector field

$$E_{\mathrm{RMF}}[\hat{\rho},\phi_m] = \mathrm{Tr}[(\boldsymbol{\alpha p}+\beta m)\hat{\rho}] \pm \int \left[\frac{1}{2}(\nabla\phi_m)^2 + U(\phi_m)\right] \mathrm{d}^3 r + \mathrm{Tr}[(\Gamma_m \phi_m)\hat{\rho}]$$

density matrix $\hat{\rho}$

$\phi_m \equiv \{\sigma, \omega^\mu, \vec{\rho}^\mu, A^\mu\}$ - meson fields

$$\hat{h} = \frac{\delta E}{\delta \hat{\rho}}$$ **Mean field**

$$\hat{h}|\varphi_i\rangle = \varepsilon_i|\varphi_i\rangle$$ **Eigenfunctions**

Motivation: better understanding of the accuracy and uncertainties in the description of different observables and how they propagate to nuclear extremes

Number of the functionals:

Skyrme	– 240	M.Dutra et al, PRC 85, 035201 (2012)
covariant functionals	-- 263,	M. Dutra et al, PRC 90, 055203 (2014)

Estimating theoretical errors:

statistical errors - well defined (not yet done)

systematic (non-statistical) errors – well defined for the regions where experimental data exist [remember "error is a deviation from true value" (webster)]

-- not well defined for the regions beyond experimentally known

Theoretical uncertainties are defined by the **spread** (the difference between maximum and minimum values of physical observable obtained with employed set of CEDF's).

$$\Delta O(Z,N) = |O_{\max}(Z,N) - O_{\min}(Z,N)|$$

NL3*, DD-ME2, DD-MEδ, DD-PC1 [also PC-PK1 in superheavy nuclei]

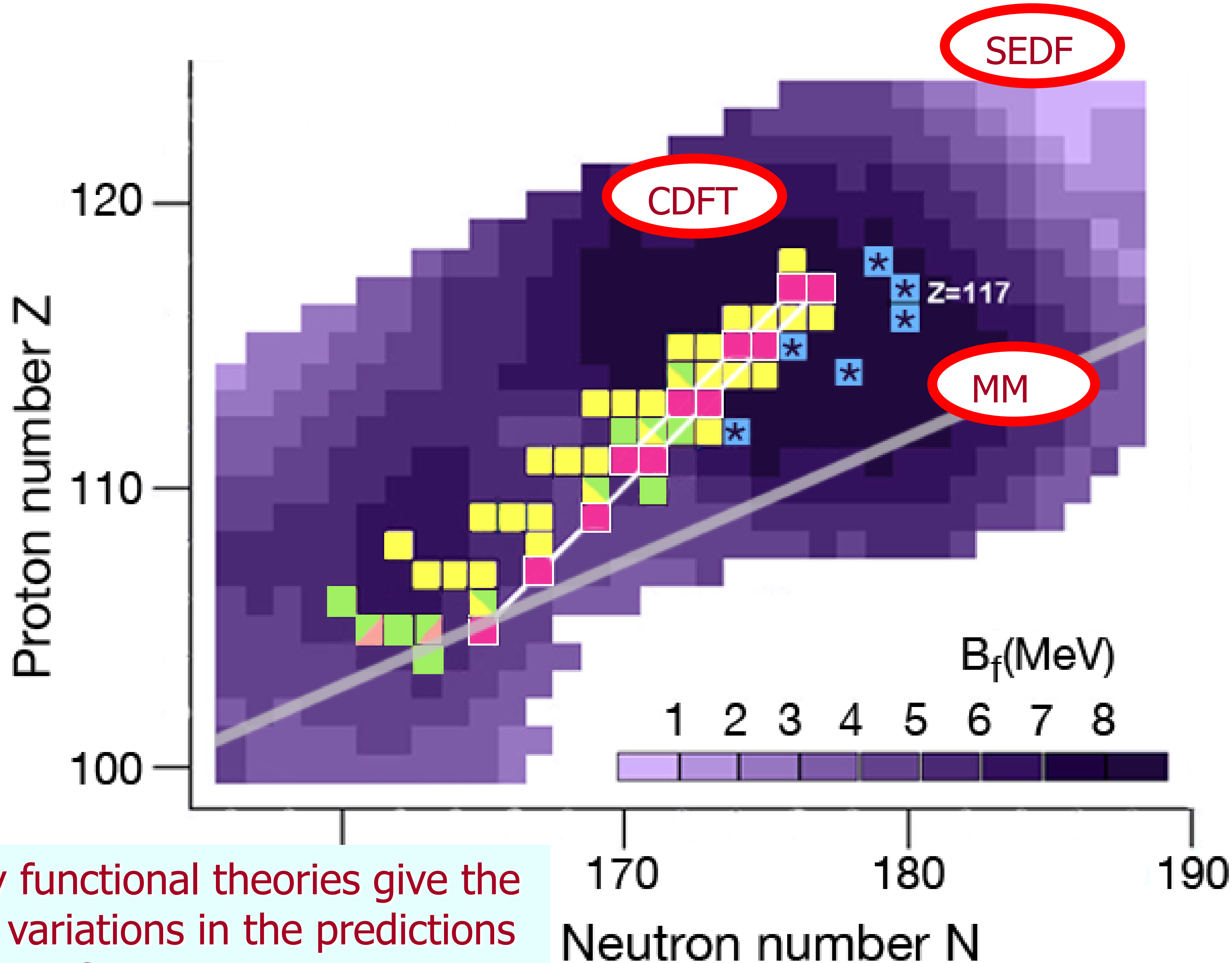

Density functional theories give the largest variations in the predictions of magic gaps

at Z=120, 126 and 172, 184

Actinides as a testing ground

Accuracy of the description of deformed one-quasiparticle states

AA and S.Shawaqfeh, PLB 706 (2011) 177

1-qp states: the comparison with non-relativistic funtionals

J. Dobaczewski, AA, M. Bender, L. Robledo, Y .Shi, Nucl. Phys. A, in press

Fission barriers in actinides and SHE

actinides: H. Abusara, AA and P. Ring, PRC 82, 044303 (2010)

superheavies: H. Abusara, AA and P. Ring, PRC 85, 024314 (2012)

Pairing and rotational properties of even-even of odd-mass actinides

AA and O.Abdurazakov, PRC 88, 014320 (2013), AA, Phys. Scr. 89 (2014) 054001

CDFT calculations for ^{252}No with the NL1 parametrization

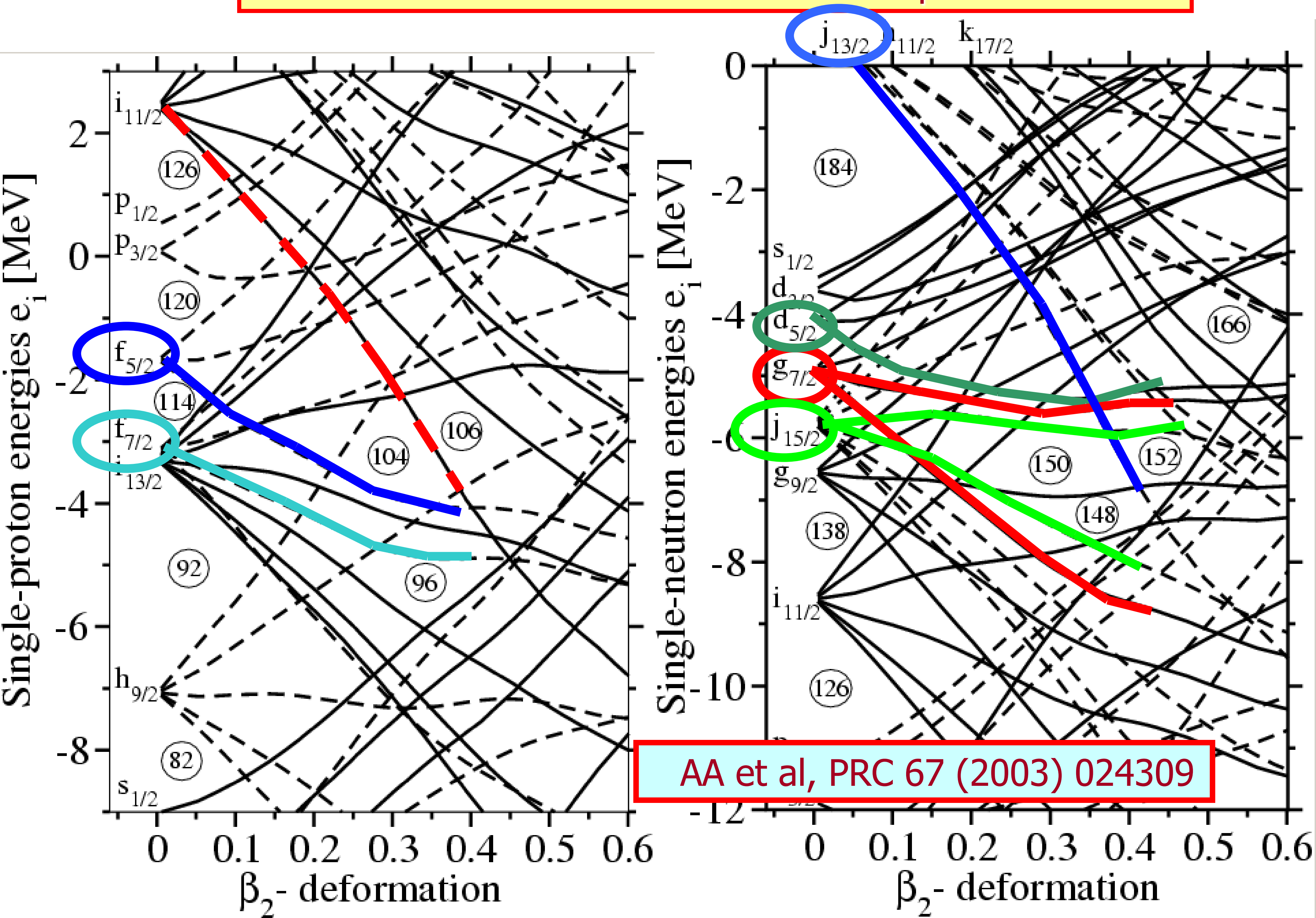

AA et al, PRC 67 (2003) 024309

Systematics of one-quasiparticle states in actinides: the CRHB study

Triaxial CRHB; fully self-consistent blocking, time-odd mean fields included, Gogny D1S pairing, AA and S.Shawaqfeh, PLB 706 (2011) 177

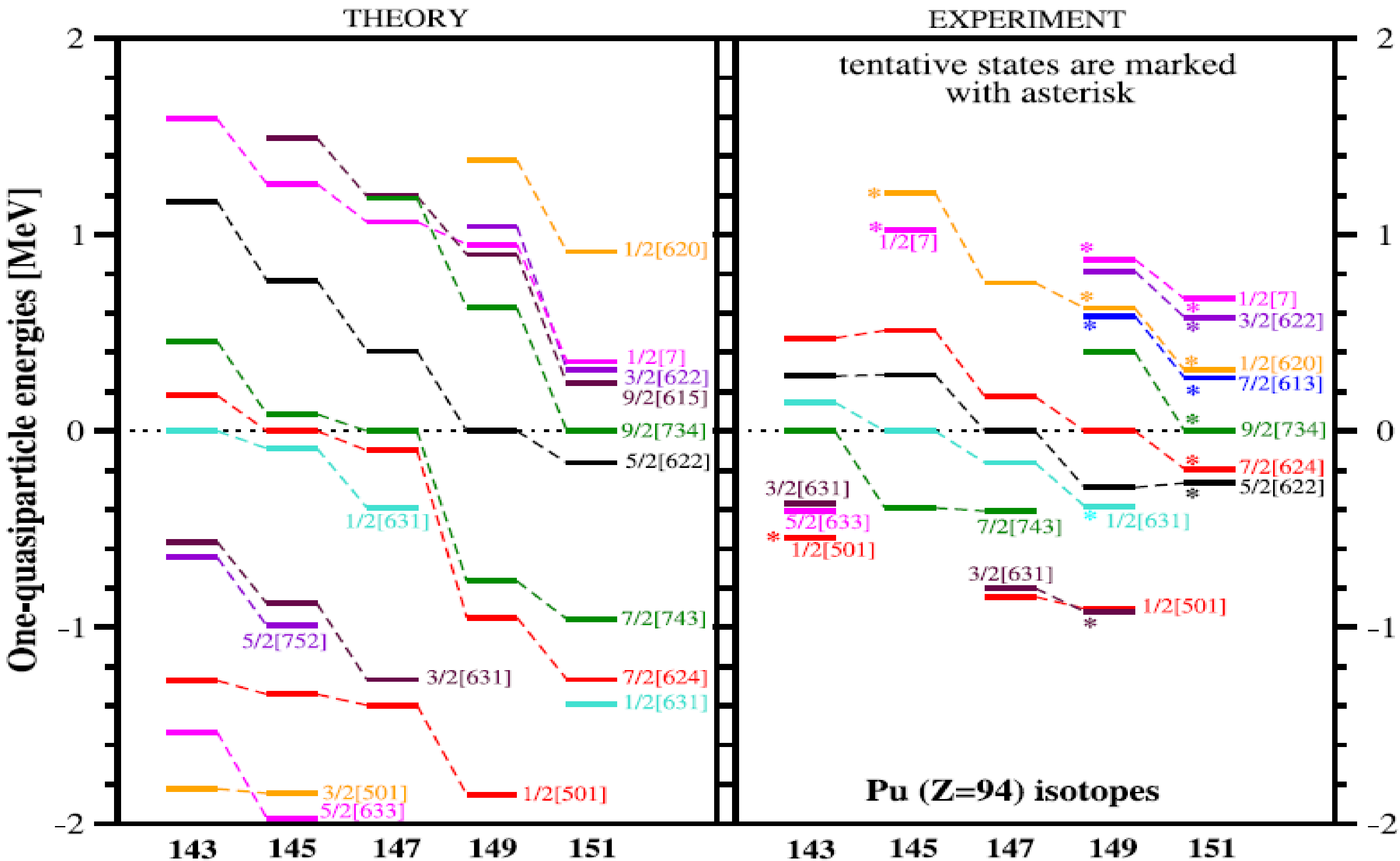

Neutron number N

Deformed one-quasiparticle states: covariant and non-relativistic DFT description versus experiment

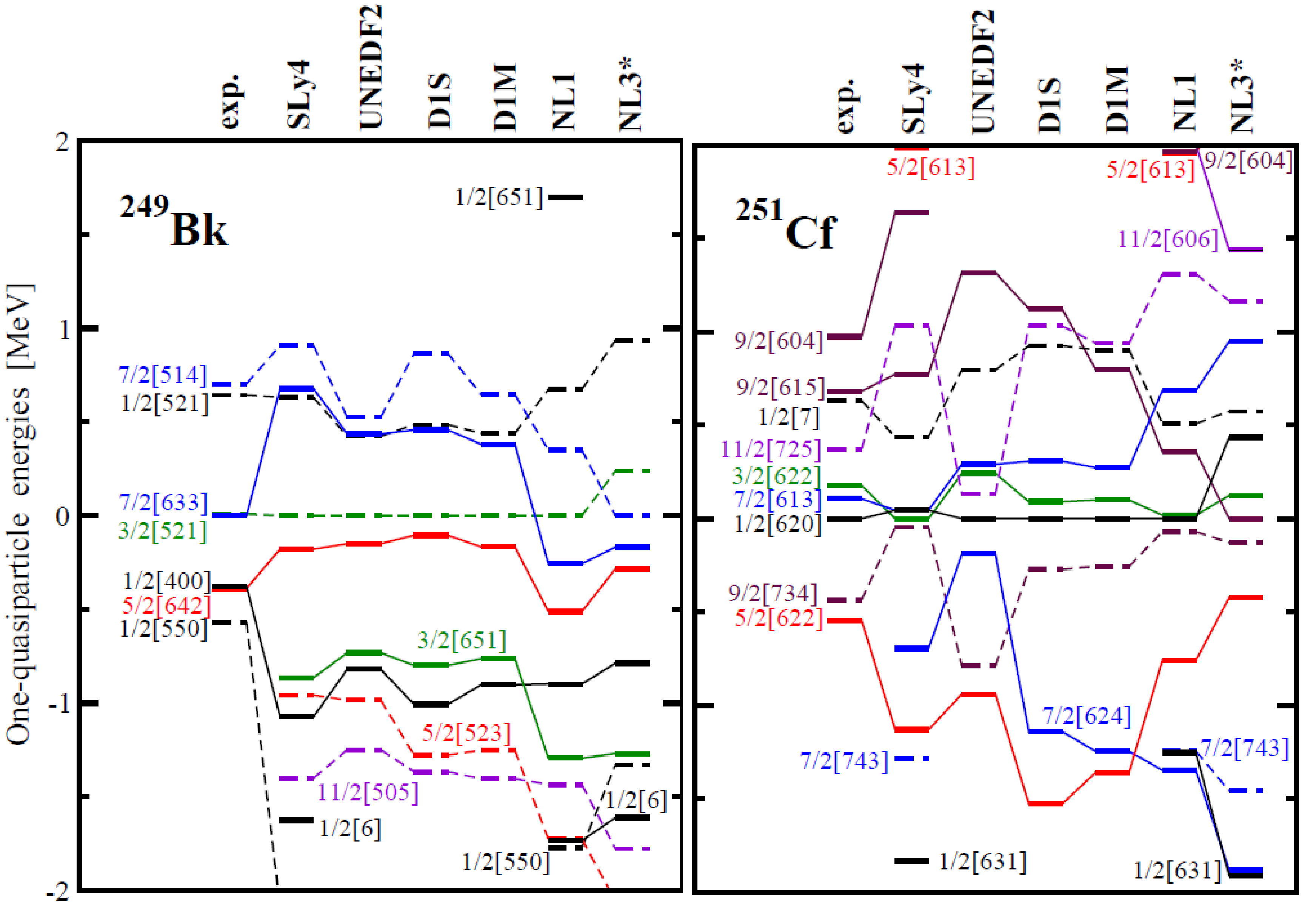

J.Dobaczewski, AA, et al, NPA, in press

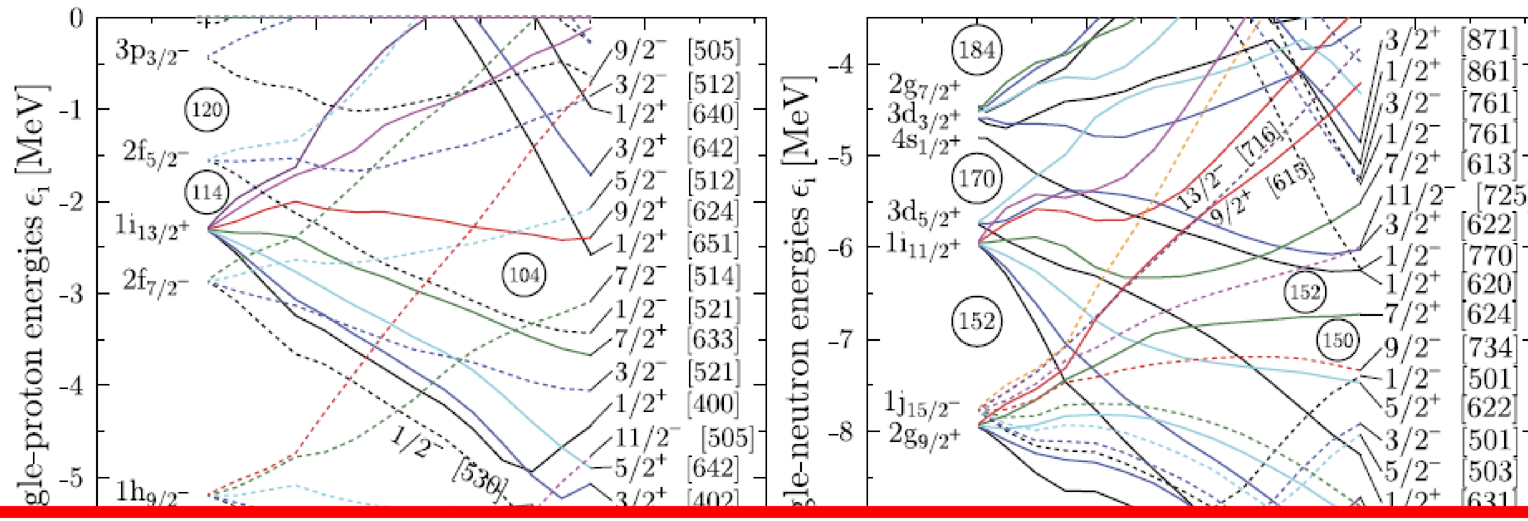

The necessary shift of the spherical shells that one would expect to correct for the disagreement between calculation and data for deformed states will not lead to similar spherical shell gaps in non-relativistic and relativistic calculations.

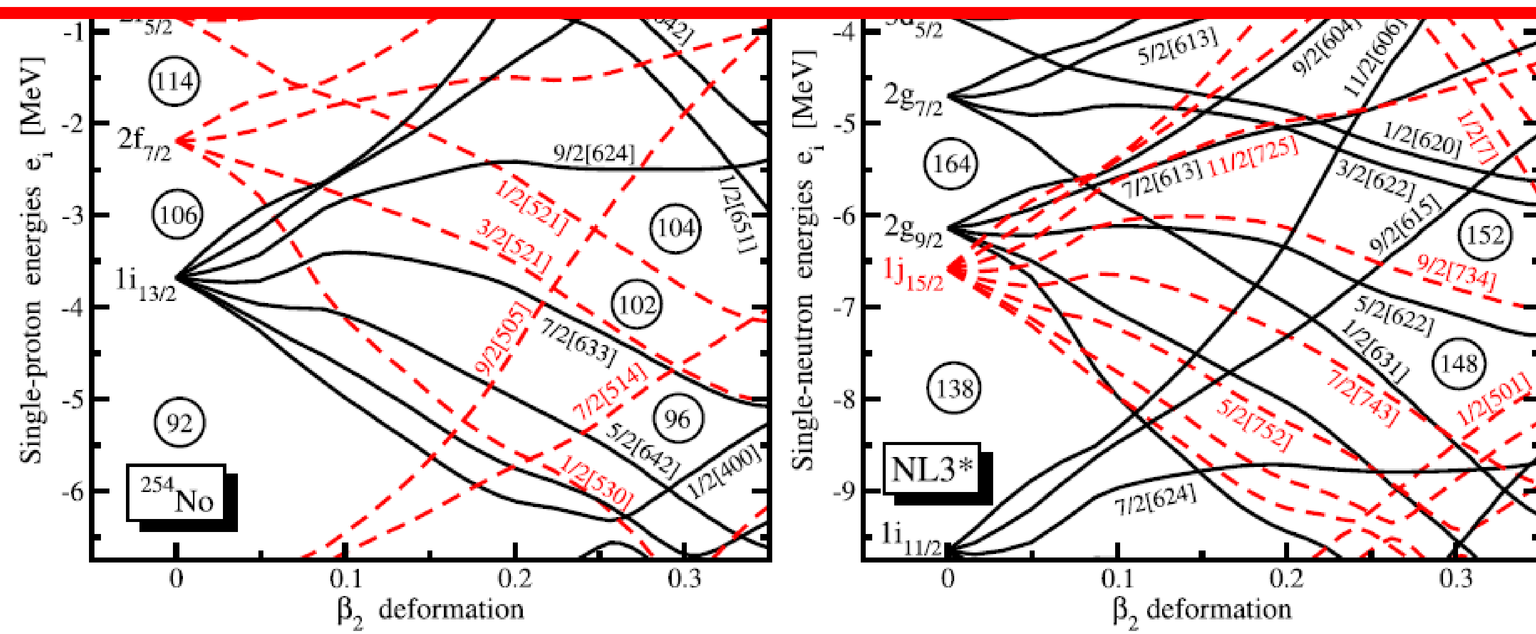

Statistical distribution of deviations of the energies of one-quasiparticle states from experiment

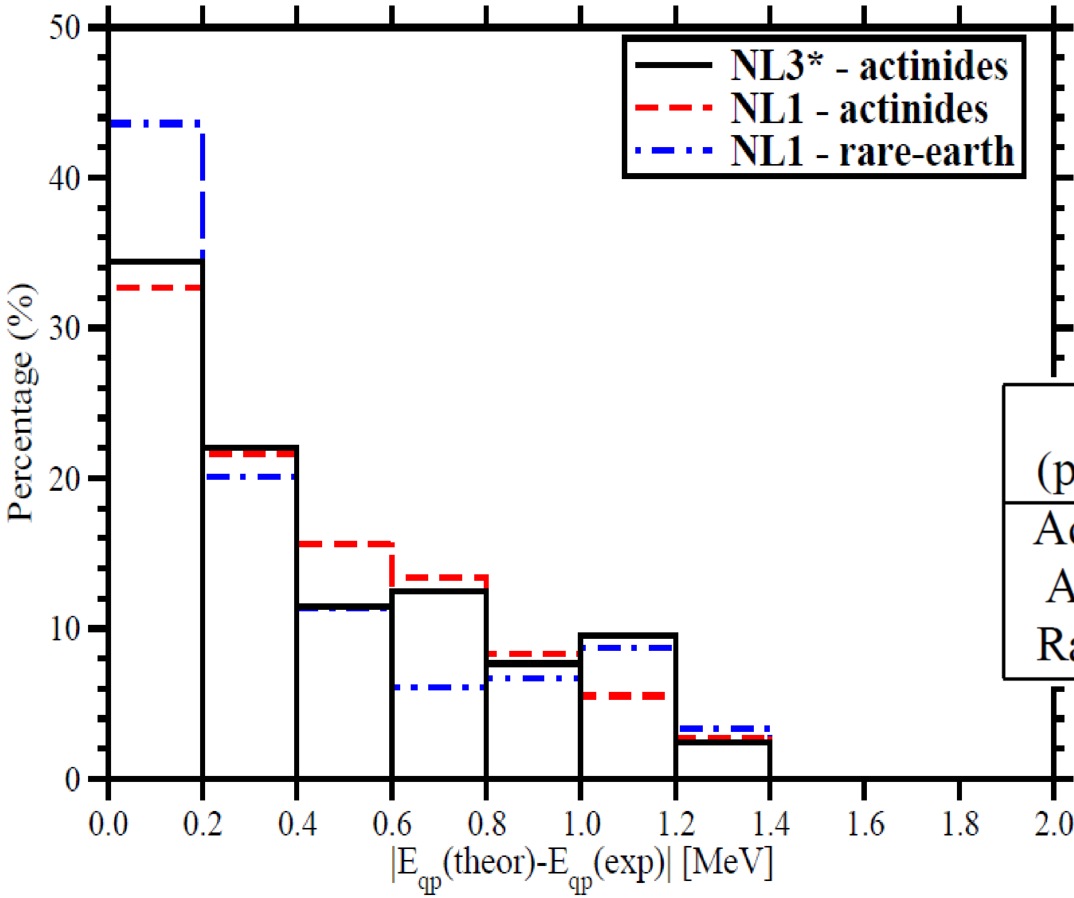

The description of deformed states at DFT level is better than spherical ones by a factor 2-3 (and by a factor ~1 (neutron) and ~2 (proton) as compared with spherical PVC calculations)

Region (parametrization)	calculated states (#)	compared states (#)
Actinides (NL3*)	415	209
Actinides (NL1)	444	217
Rare-earth (NL1)	360	149

Triaxial CRHB; fully self-consistent blocking, time-odd mean fields included, NL3*, Gogny D1S pairing, AA and S.Shawaqfeh, PLB 706 (2011) 177

Two sources of deviations:

1. Low effective mass (stretching of the energy scale)
2. Wrong relative energies of some states

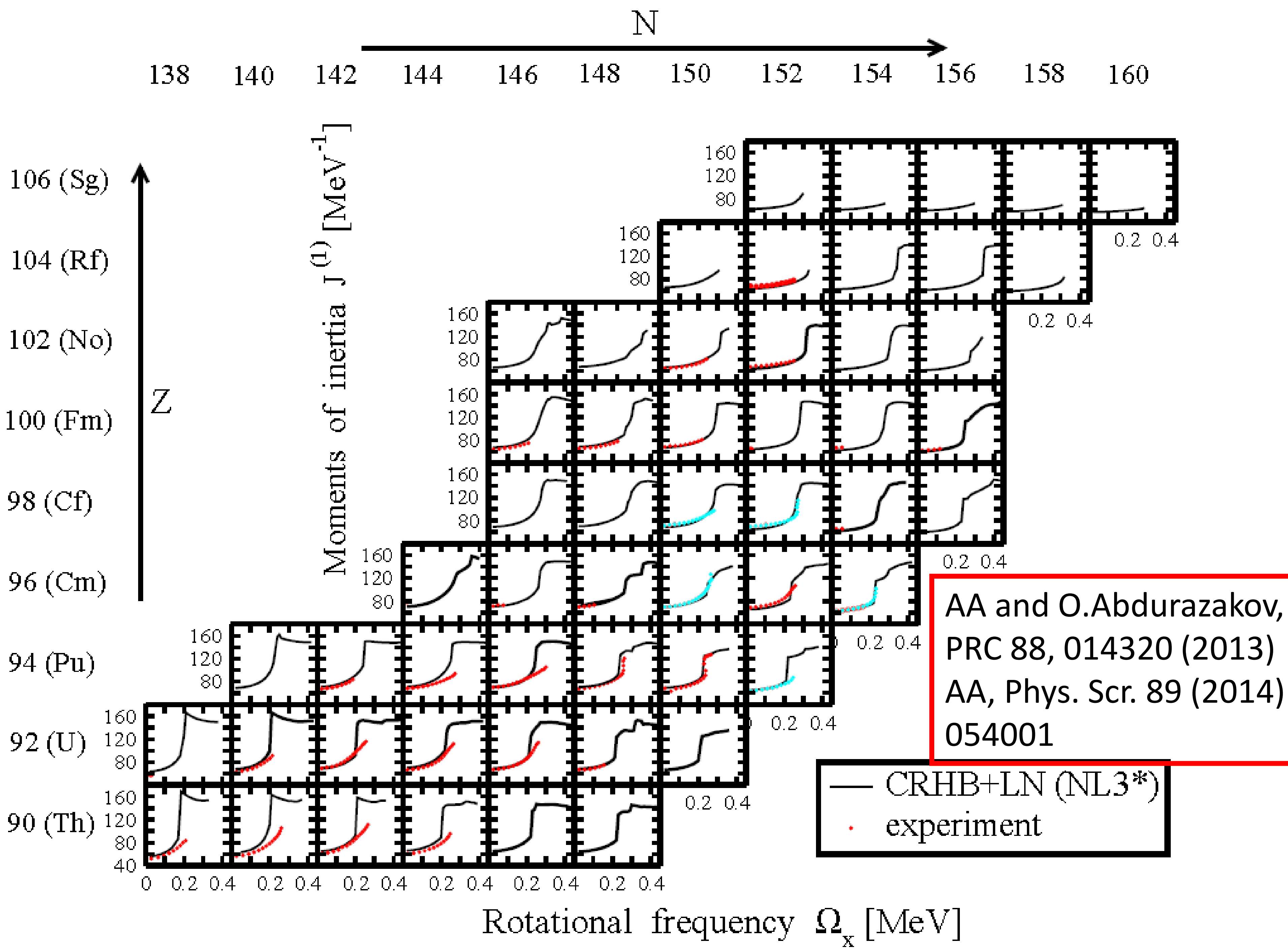
N
138 140 142 144 146 148 150 152 154 156 158 160
Z
106 (Sg)
104 (Rf)
102 (No)
100 (Fm)
98 (Cf)
96 (Cm)
94 (Pu)
92 (U)
90 (Th)
Moments of inertia $J^{(1)}$ [MeV^{-1}]
Rotational frequency Ω_x [MeV]
AA and O.Abdurazakov, PRC 88, 014320 (2013)
AA, Phys. Scr. 89 (2014) 054001
CRHB+LN (NL3*)
experiment

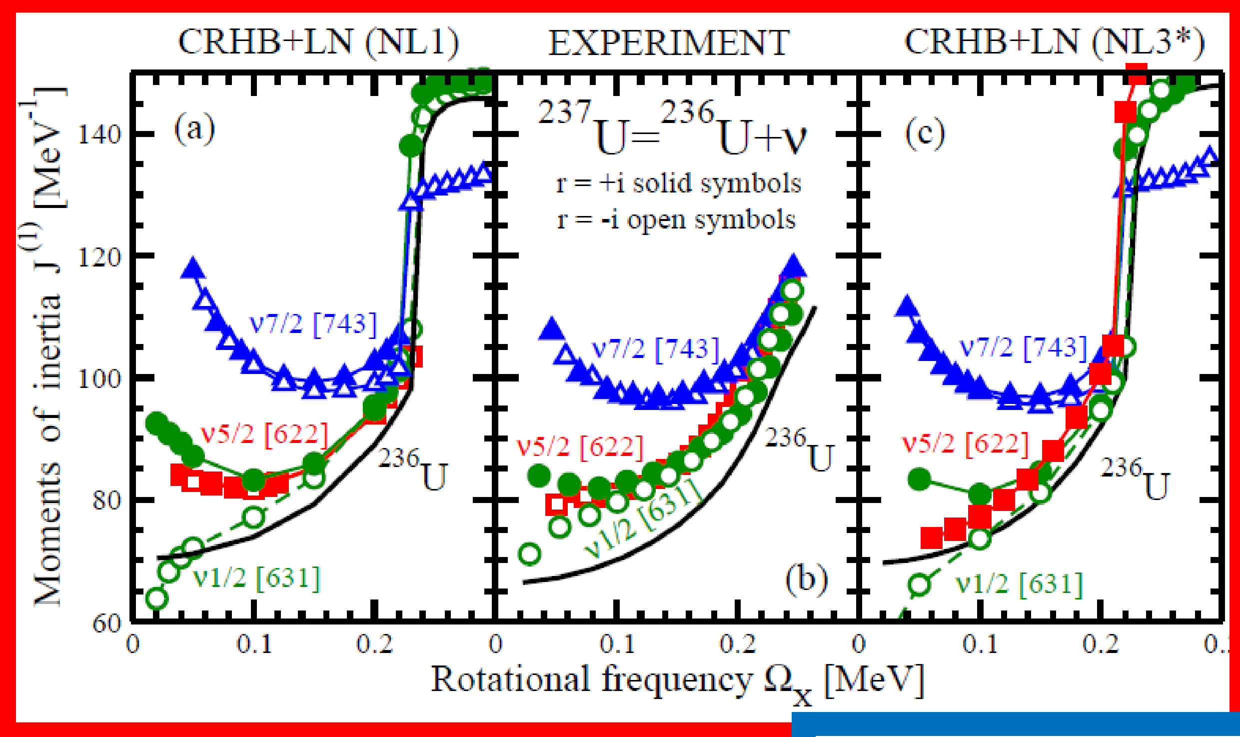

Increase of $J^{(1)}$ in odd-proton nucleus as compared with even-even ^{240}Pu is due to blocking which includes:

(a) Decrease of proton or neutron pairing

(b) Alignment properties of blocked proton or neutron state

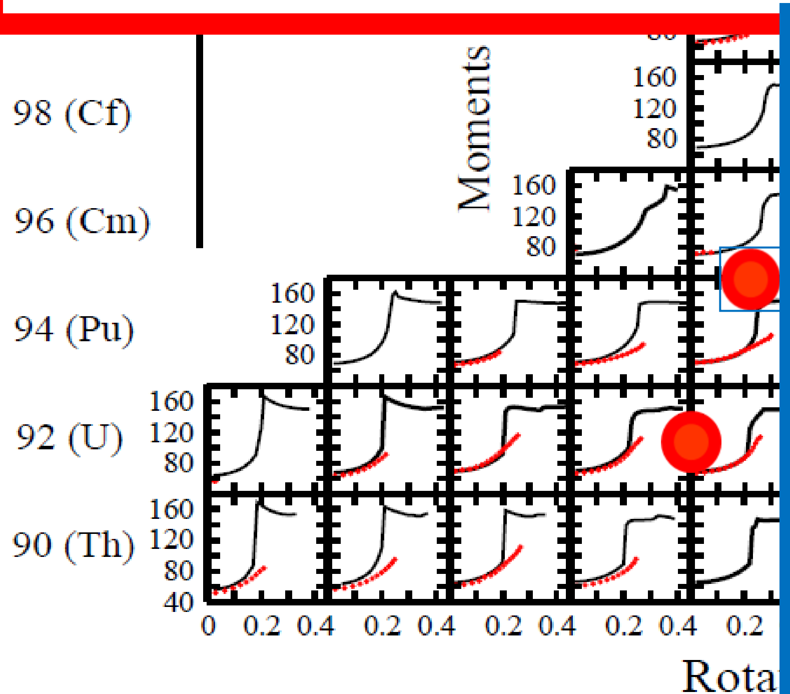

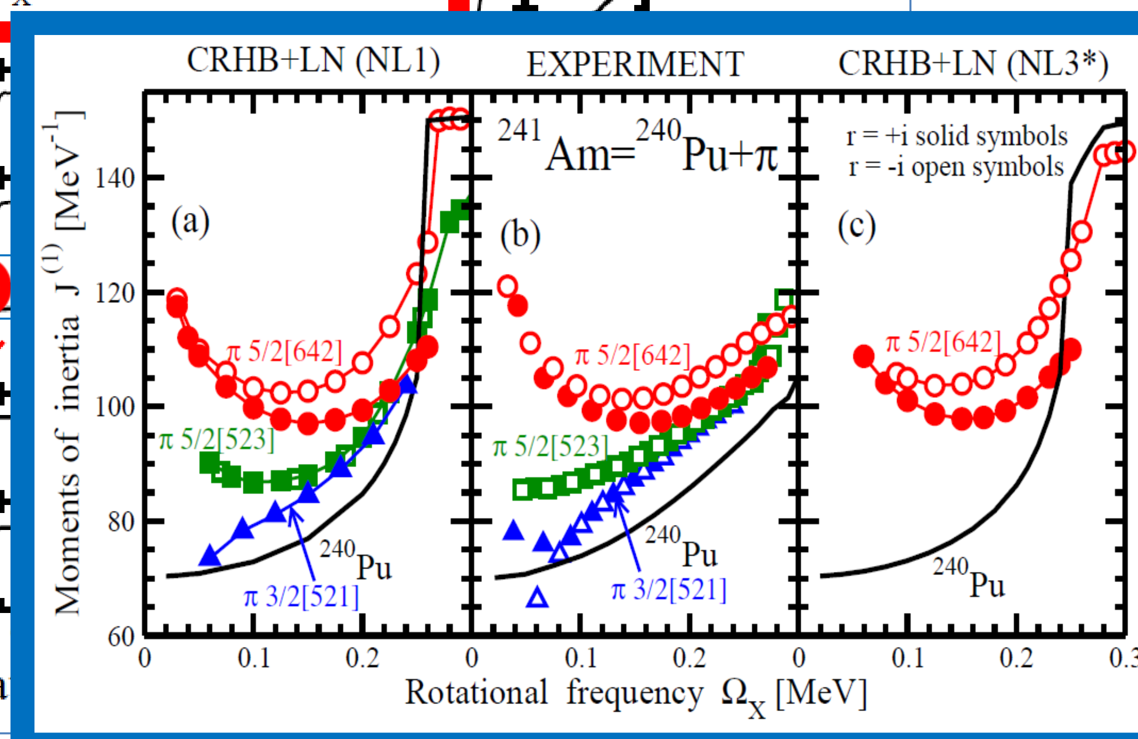

Paired band crossings: CRHB+LN versus CSM+PNP

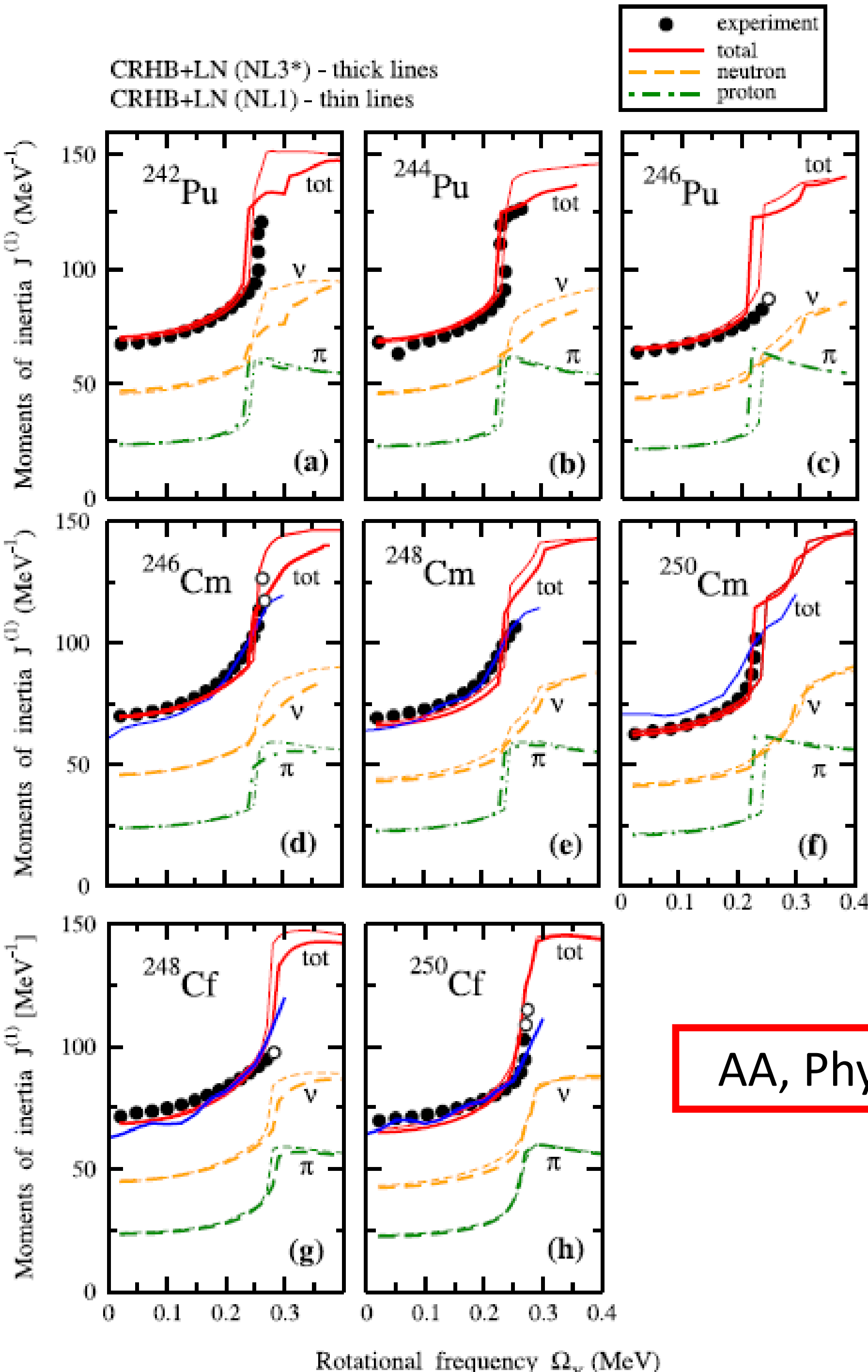

New exp. data
S. Hota, PLB 739, 13 (2014)

CSM+PNP (Z.-H.Zhang et al, PRC 85, 014324 (2012)).
Careful fit of:

- Parameters of Nilsson potential to the energies of the single-particle states
- Different pairing strength in even-even and odd nuclei
- Experimental deformations

AA, Phys. Scr. 89 (2014) 054001

CRHB+LN provides more consistent and more accurate description of experimental data than CSM+PNP

Spectroscopy of ^{240}U

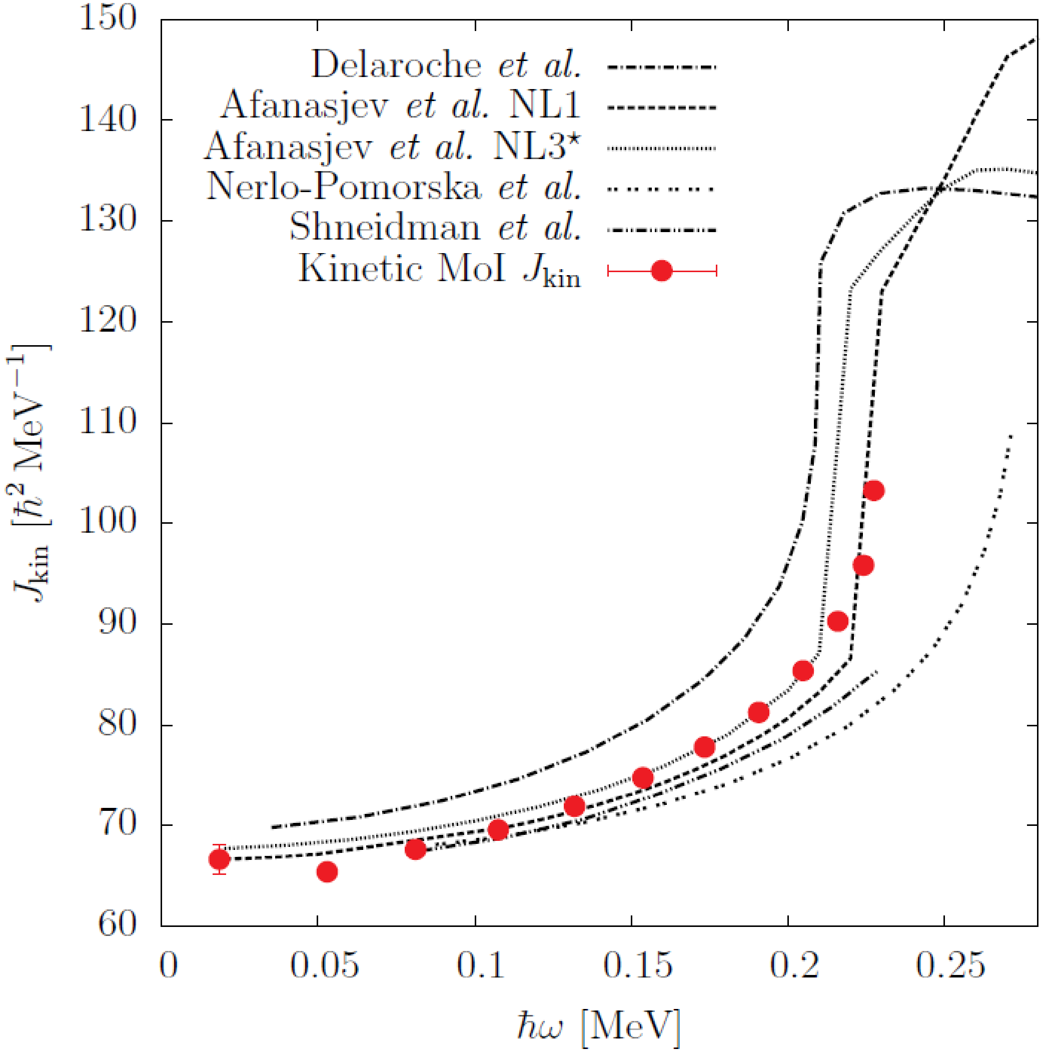

B. Birkenbah et al, Phys. Rev. C 92, 044319 (2015)

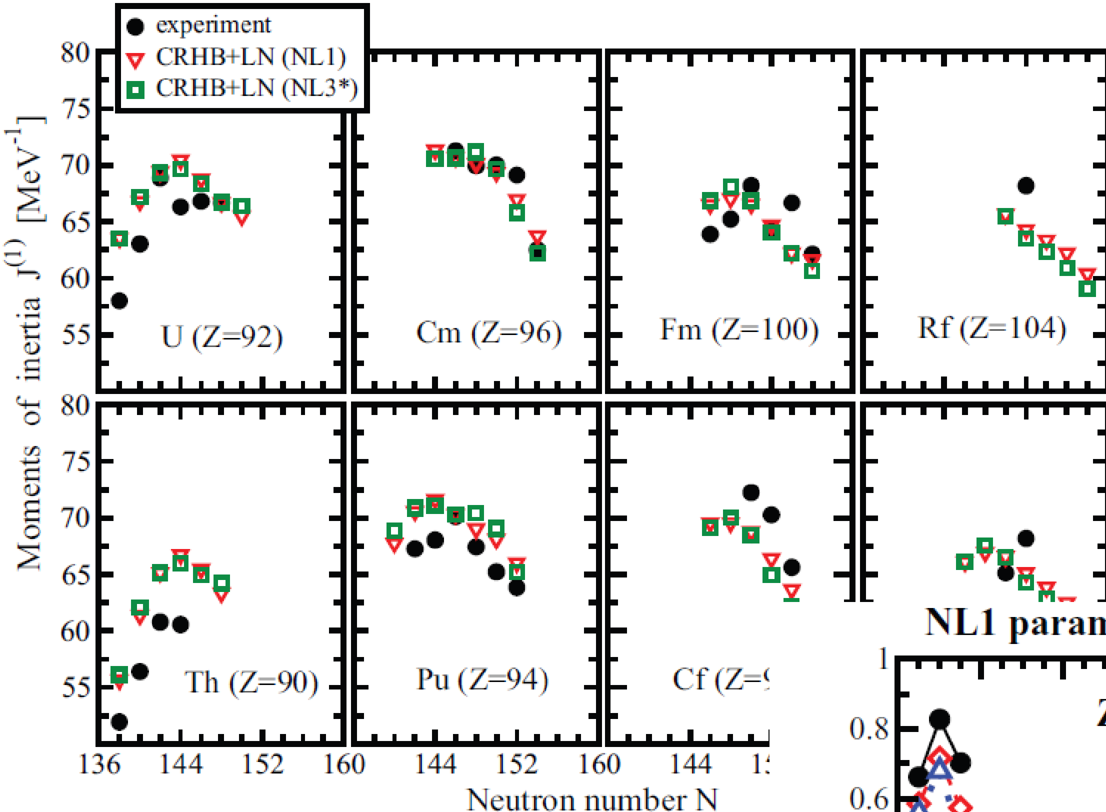

The strength of pairing defined by means of the moments of inertia and three-point $\Delta^{(3)}$ indicators strongly correlate

$$\Delta_{\nu}^{(3)}(N) = \frac{\pi_N}{2}\left[B(N-1) + B(N+1) - 2B(N)\right]$$

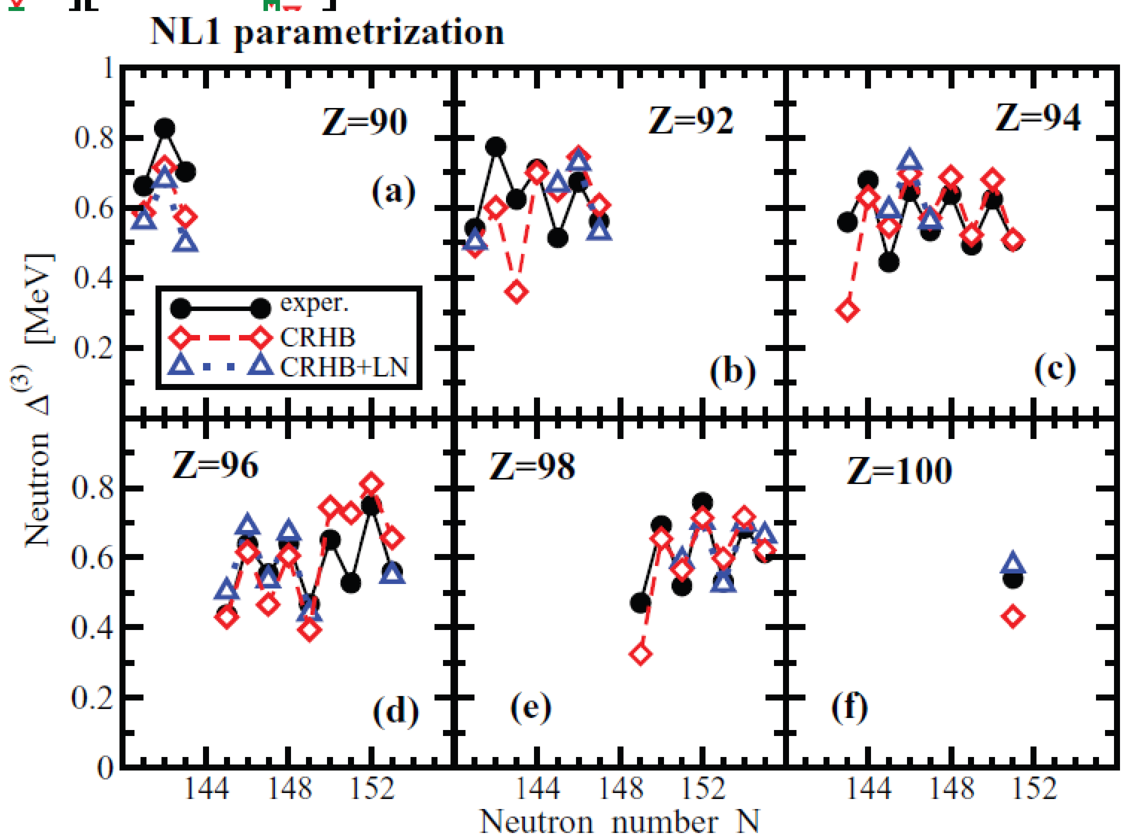

Fission barriers: theory versus experiment [state-of-the-art]

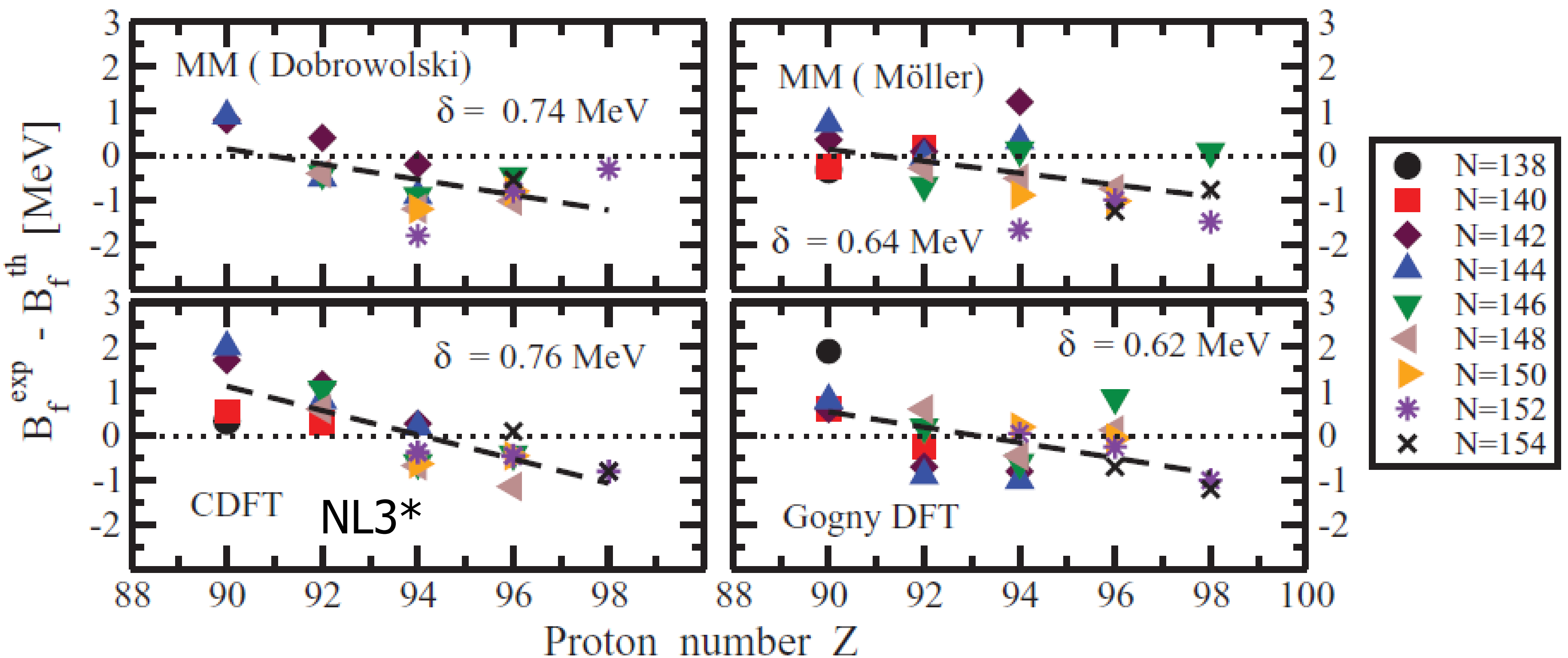

Mac+mic, LSD model A.Dobrowolski et al, PRC 75, 024613 (2007)

Mac+mic, FRDM model P. Moller et al, PRC 79, 064304 (2009)

Gogny DFT, J.-P. Delaroche et al, NPA 771, 103 (2006).

CDFT : actinides H. Abusara, AA and P. Ring, PRC 82, 044303 (2010)
superheavies: H. Abusara, AA and P. Ring, PRC 85, 024314 (2012)

No fit of functionals (parameters) to fission barriers or fission isomers only in mac+mic (Kowal) and CDFT

Bing-Ban Lu et al,
PRC **85**, 011301(R) (2012)
RMF+BCS based on PC-PK1

V. Prassa et al, PRC **86**, 024317 (2012)
RMF+BCS based on DD-PC1

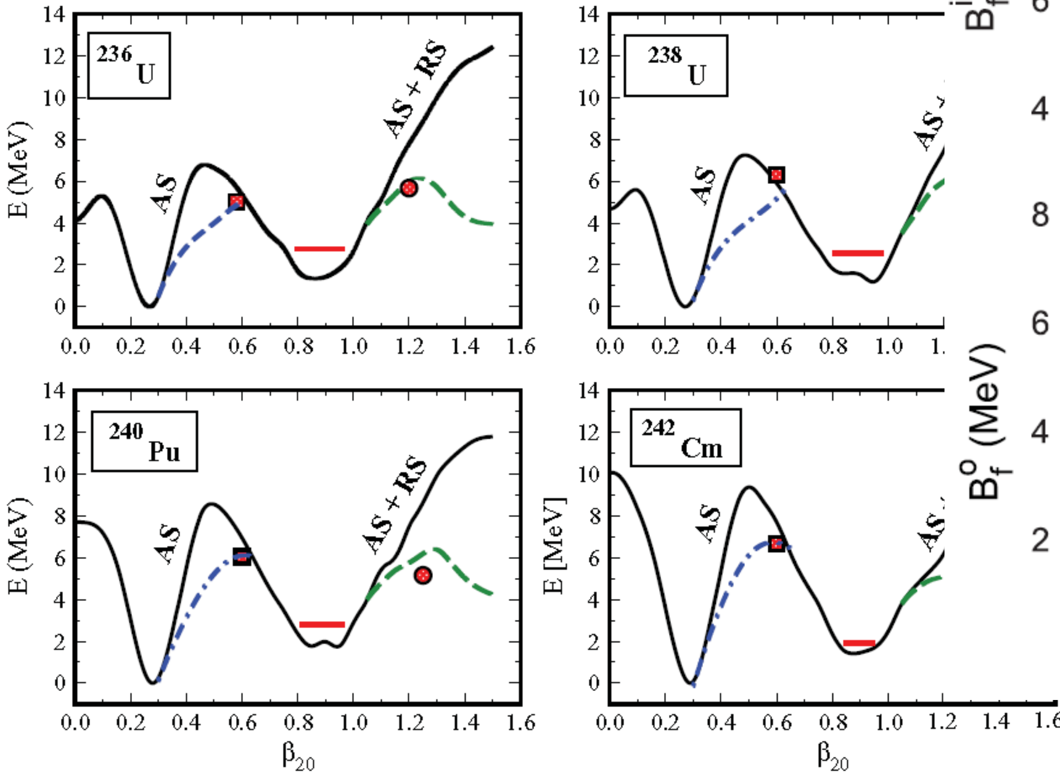

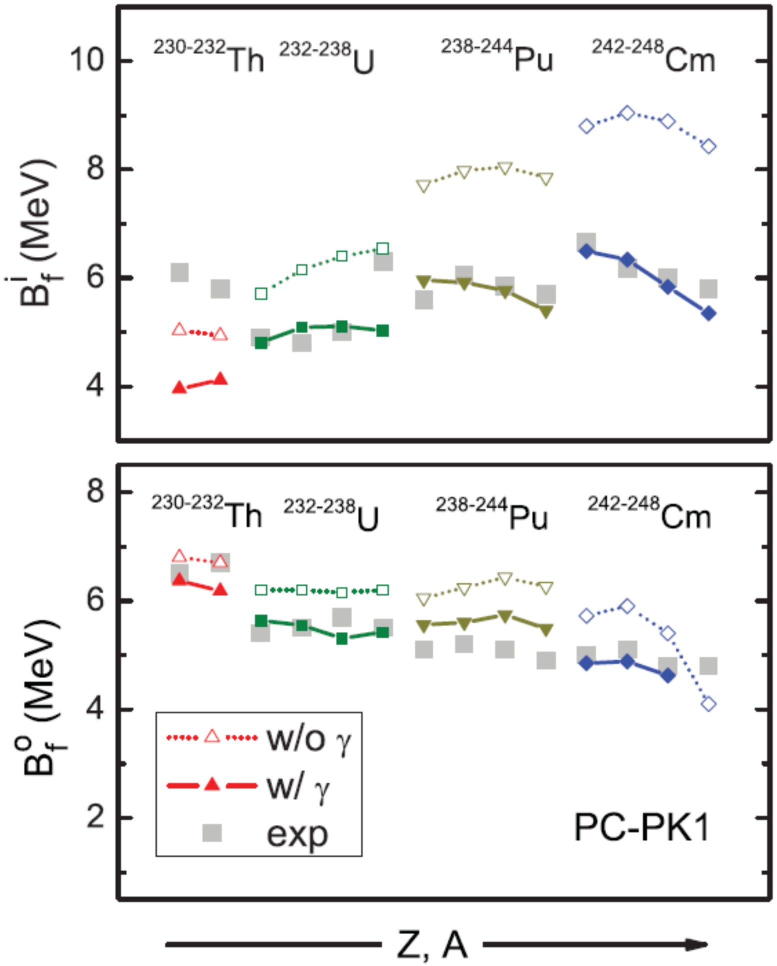

FIG. 2. (Color online) Constrained energy curves of ^{236,238}U, ^{240}Pu, and ^{242}Cm, as functions of the axial quadrupole deforma
sults of self-consistent axially and reflection-symmetric, triaxial, and axially reflection-asymmetric RMF + BCS calculations

Global performance of the state-of-the-art covariant energy density functionals

Ground state observables and estimate of theoretical uncertainties in their description: S.E.Agbemava, AA, D.Ray and P.Ring, PRC **89**, 054320 (2014) (37 pages)

- masses, separation energies, charge radii, neutron skins, two-proton and two-neutron drip lines
- includes as a supplement to the manuscript **complete mass table for even-even nuclei with Z<104 obtained with DD-PC1**

Neutron drip lines and sources of their uncertainties:

PLB 726, 680 (2013), PRC **89**, 054320 (2014) , PRC 91, 014324 (2015)

RHB framework

$$\begin{pmatrix} h_D - \lambda & \Delta \\ -\Delta^* & -h_D^* + \lambda \end{pmatrix} \begin{pmatrix} U \\ V \end{pmatrix}_k = E_k \begin{pmatrix} U \\ V \end{pmatrix}_k$$

1. Axial RHB calculations in large basis (all fermionic states up to N_F=20 and bosonic states up to N_B=20 are included)

2. The separable version of the finite range Brink-Booker part of the Gogny D1S force is used in the particle-particle channel; its strength variation across the nuclear chart is defined by means of the fit of rotational moments of inertia calculated in the cranked RHB framework to experimental data.

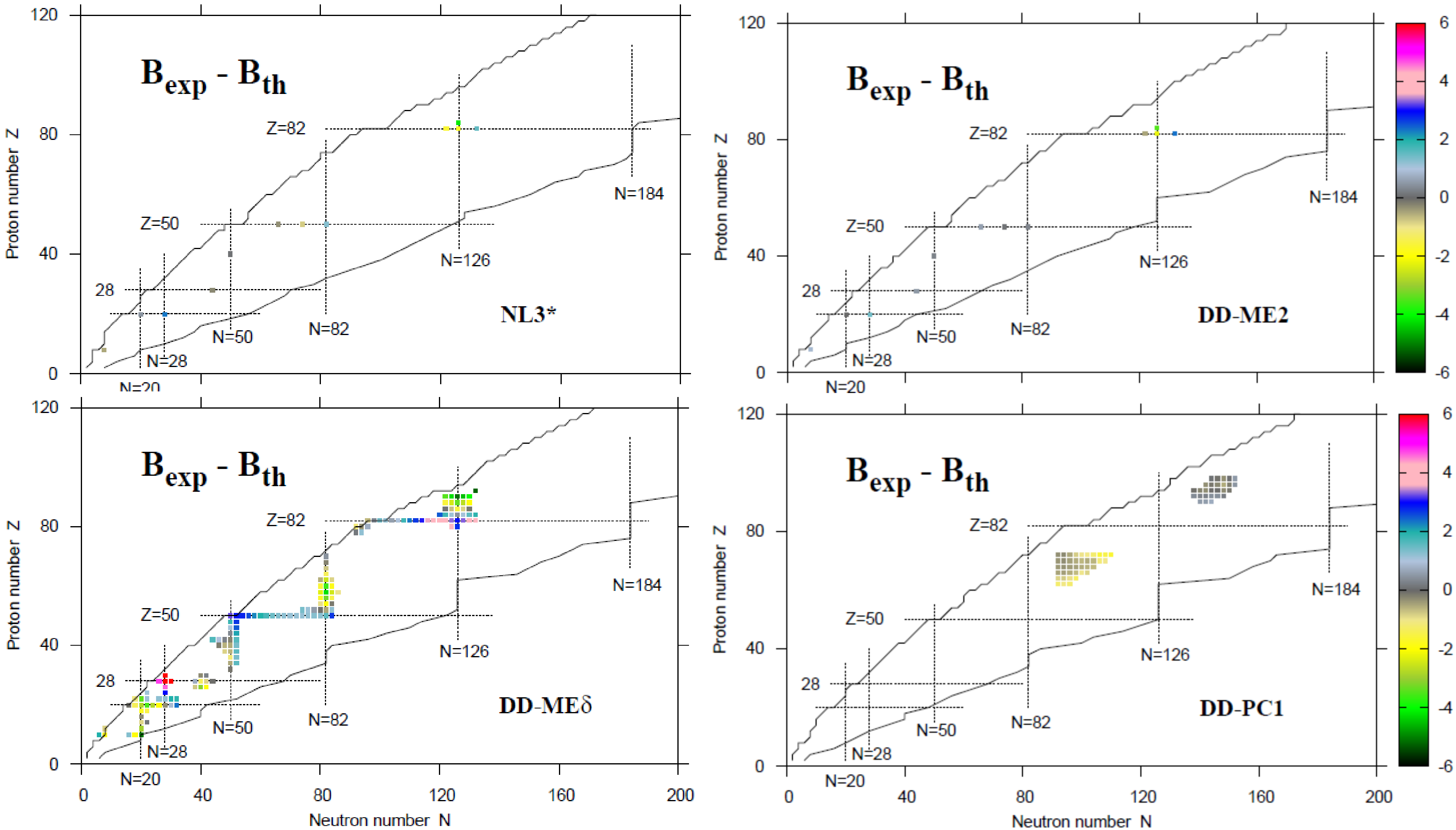

NL3* - G.A. Lalazissis et al PLB 671 (2009) 36 - **7 parameters**

DD-ME2 - G. A. Lalazissis, et al, PRC **71**, 024312 (2005) – **10 parameters**

DD-PC1 - T. Niksic et al, PRC **78**, 034318 (2008) – **10 parameters**

DD-Meδ - X. Roca-Maza et al, PRC **84**, 054309 (2011) – **14 parameters**

only 4 parameters are fitted to finite nuclei,

others - to Bruckner calculations of nuclear matter

What are theoretical uncertainties in the description of experimental masses

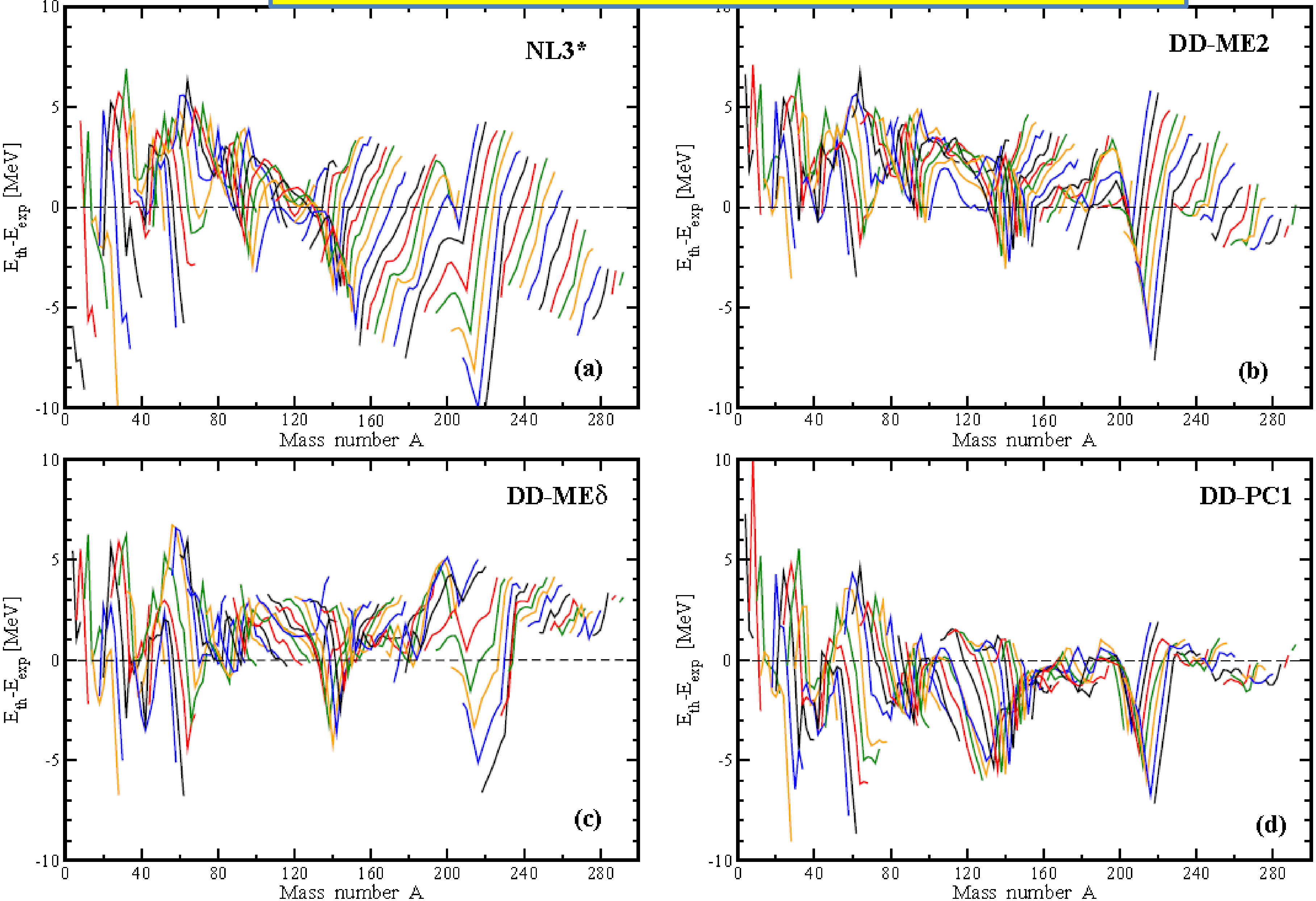

Theoretical uncertainties in the description of masses

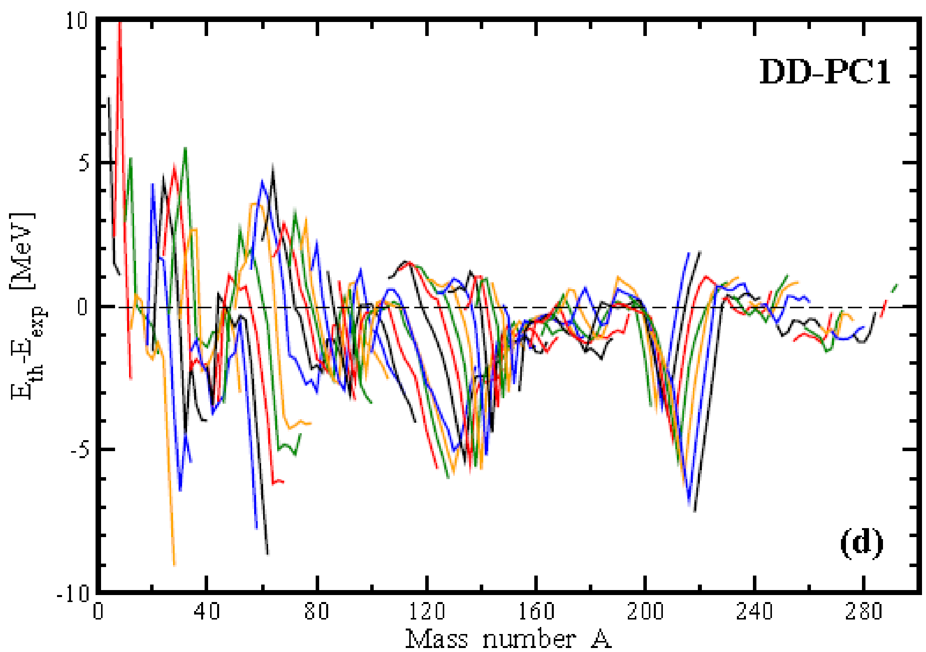

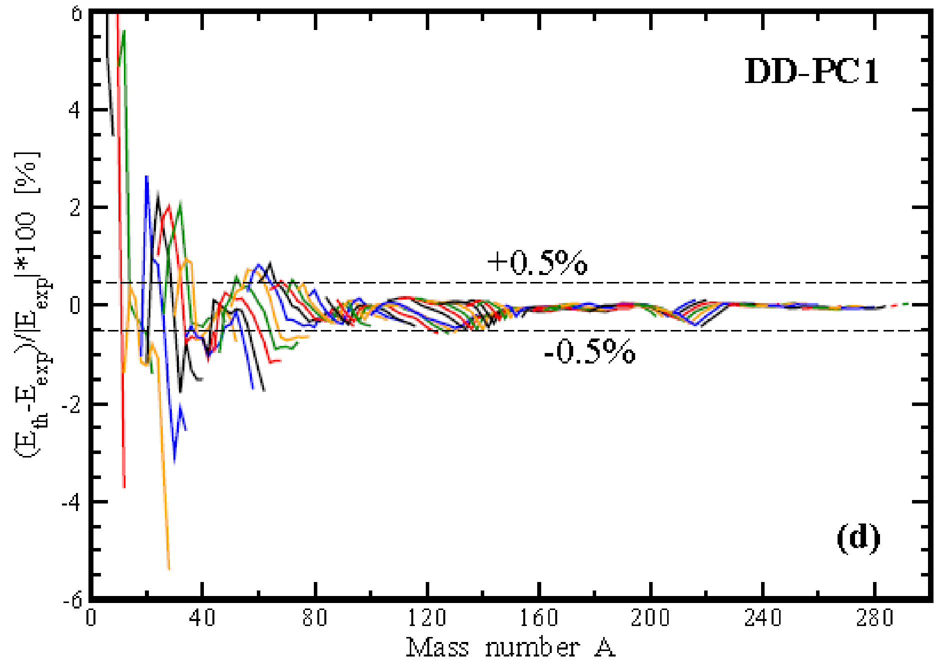

EDF	measured	measured+estimated		
	$\Delta E_{\rm rms}$	$\Delta E_{\rm rms}$	$\Delta(S_{2n})_{\rm rms}$	$\Delta(S_{2p})_{\rm rms}$
NL3*	2.96	3.00	1.23	1.29
DD-ME2	2.39	2.45	1.05	0.95
DD-MEδ	2.29	2.40	1.09	1.09
DD-PC1	2.01	2.15	1.16	1.03

Uncertainties in radii

CEDF	Δr_{ch}^{rms} [fm]
NL3*	0.0283
DD-ME2	0.0230
DD-MEd	0.0329
DD-PC1	0.0253

S. Agbemava, AA, D, Ray, P.Ring, PRC **89**, 054320 (2014) includes complete DD-PC1 mass table as supplement

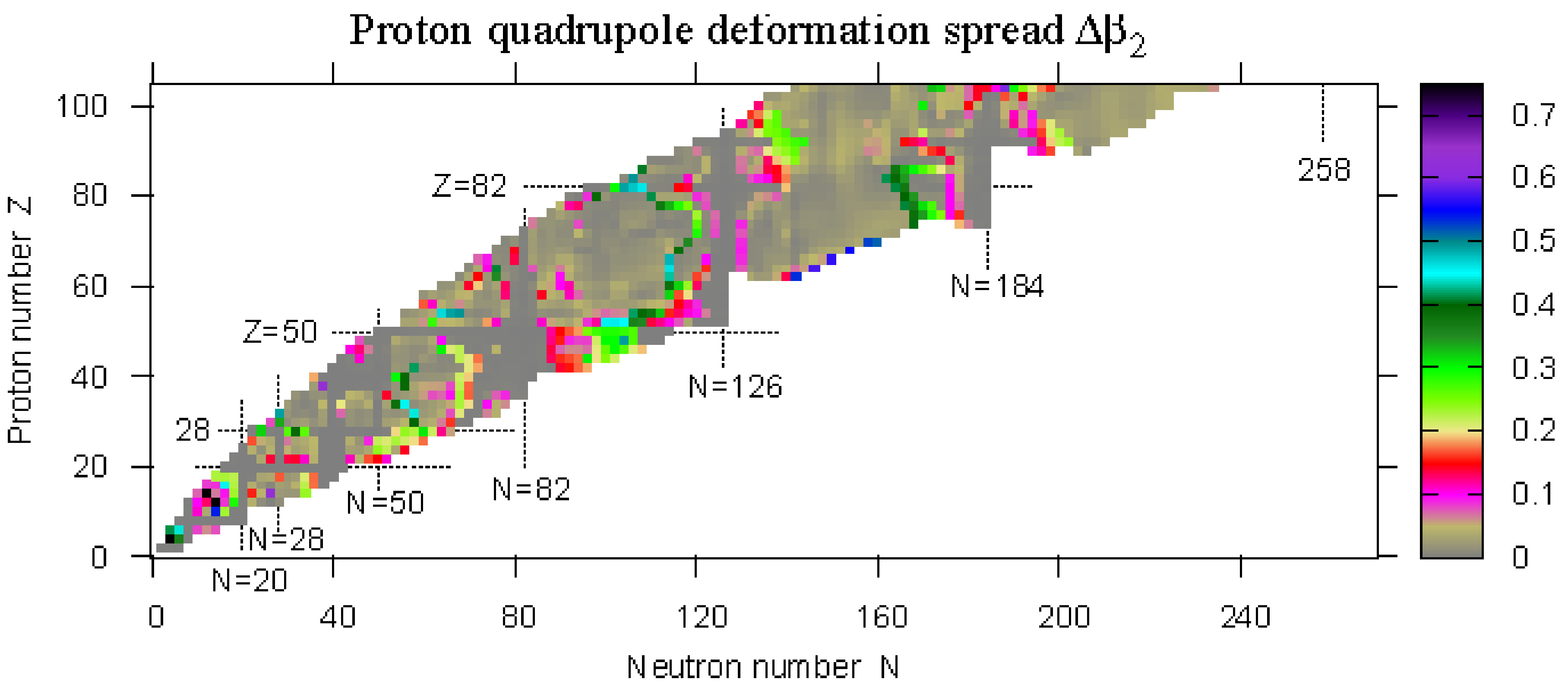

Theoretical uncertainties are most pronounced for transitional nuclei (due to soft potential energy surfaces) and in the regions of transition between prolate and oblate shapes. Details depend of the description of single-particle states

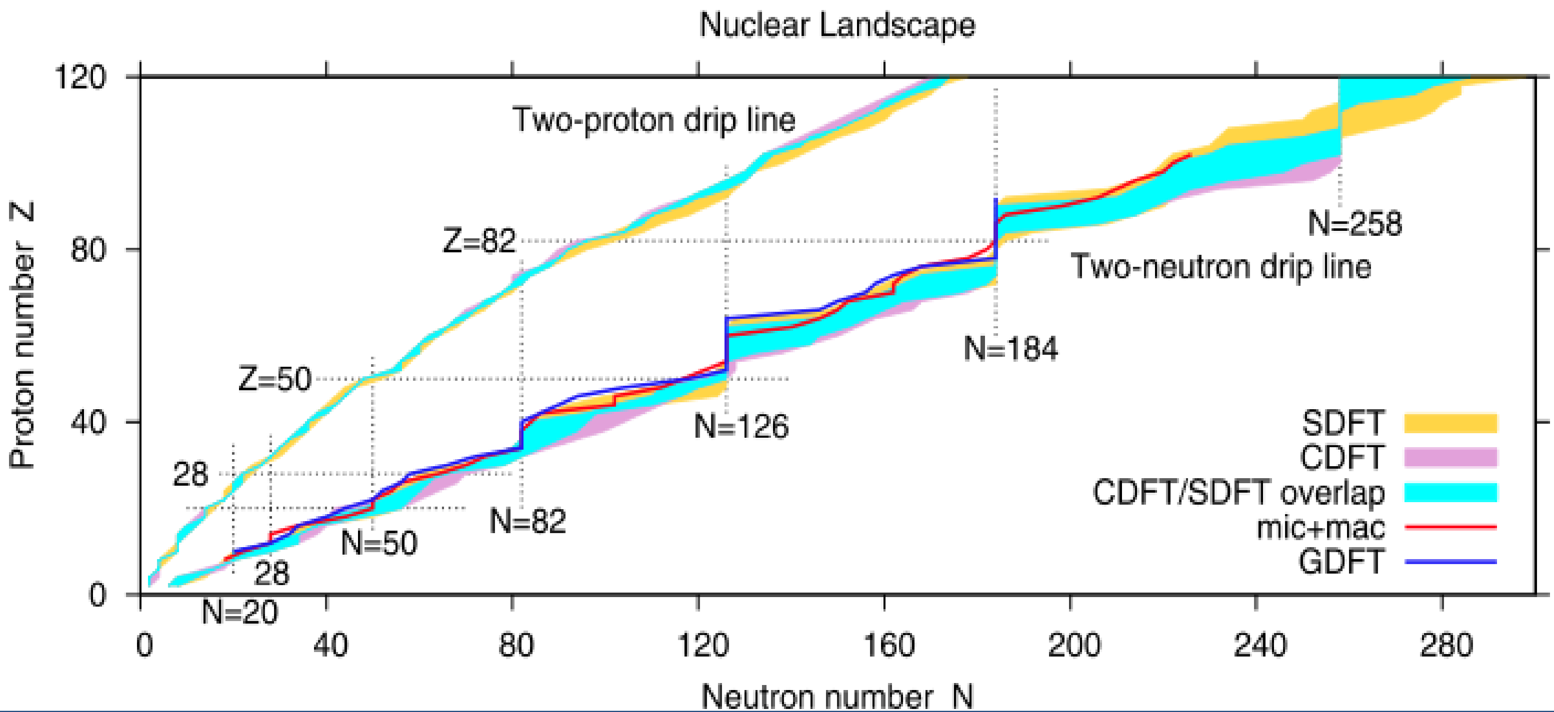

Sources of uncertainties in the prediction of two-neutron drip line

--- **poorly known isovector properties of energy density functionals** (**the position of two-neutron drip line does not correlate with nuclear matter properties of the energy density functional** (PLB 726, 680 (2013), PRC 85, 014324 (2014))

--- **inaccurate description of energies of the single-particle states** (PRC 91, 014324 (2015),

--- **shallow slope of two-neutron separation energies** (PRC 85, 014324 (2014))

Extrapolation to superheavy nuclei

S. Agbemava, AA, T. Nakatsukasa and P. Ring, PRC in press,
will appear this week

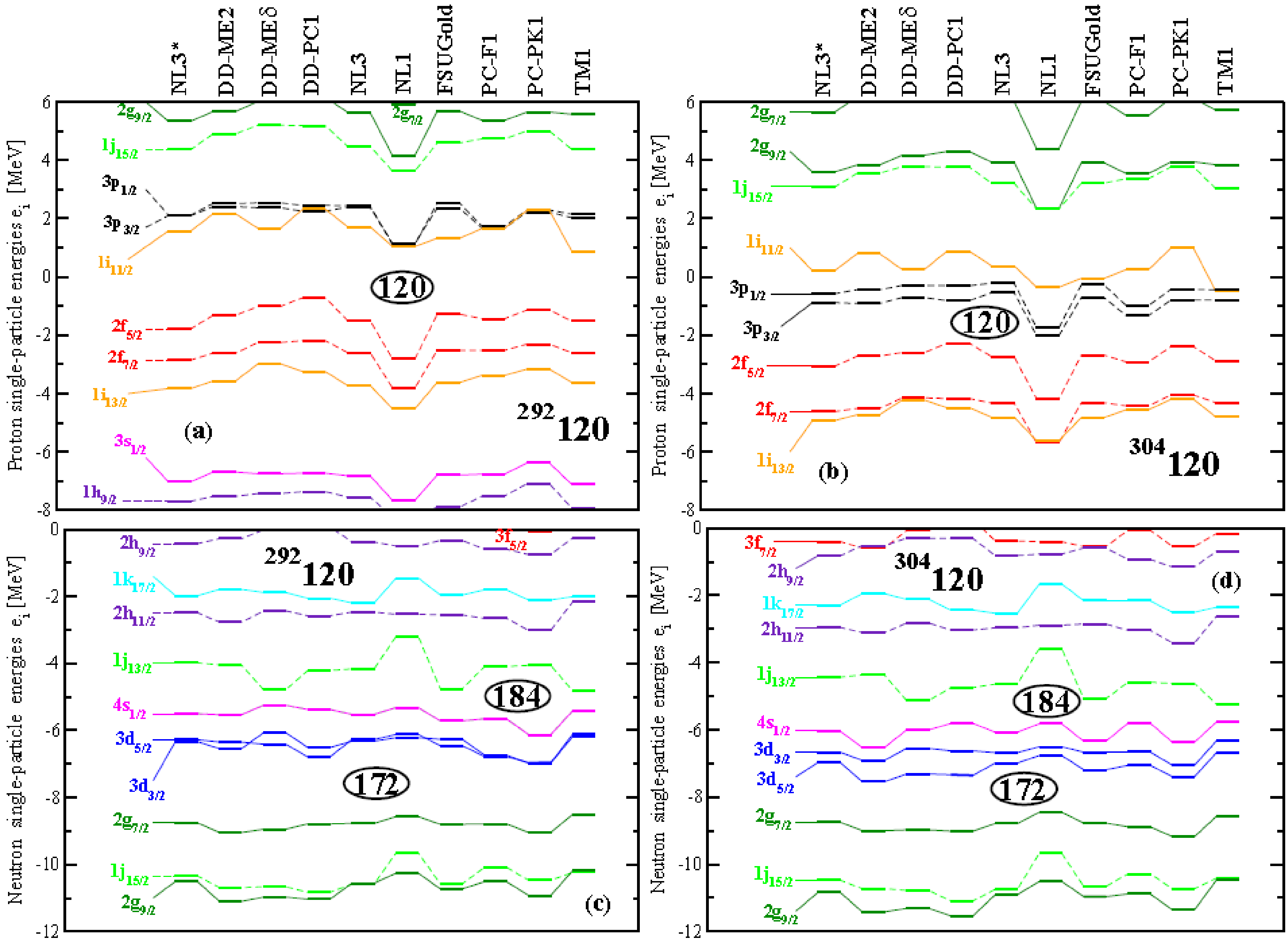

NL3*
DD-ME2
DD-MEδ
DD-PC1
NL3
NL1
FSUGold
PC-F1
PC-PK1
TM1
Proton single-particle energies e_i [MeV]
$2g_{9/2}$
$2g_{7/2}$
$1j_{15/2}$
$3p_{1/2}$
$3p_{3/2}$
$1i_{11/2}$
120
$2f_{5/2}$
$2f_{7/2}$
$1i_{13/2}$
(a)
$^{292}120$
$3s_{1/2}$
$1h_{9/2}$
(b)
$^{304}120$
Neutron single-particle energies e_i [MeV]
$2h_{9/2}$
$3f_{5/2}$
$3f_{7/2}$
$1k_{17/2}$
$2h_{11/2}$
$1j_{13/2}$
184
$4s_{1/2}$
$3d_{5/2}$
$3d_{3/2}$
172
$1j_{15/2}$
(c)
(d)
6
4
2
0
-2
-4
-6
-8
-10
-12

Theoretical uncertainties in the prediction of the sizes of shell gaps.

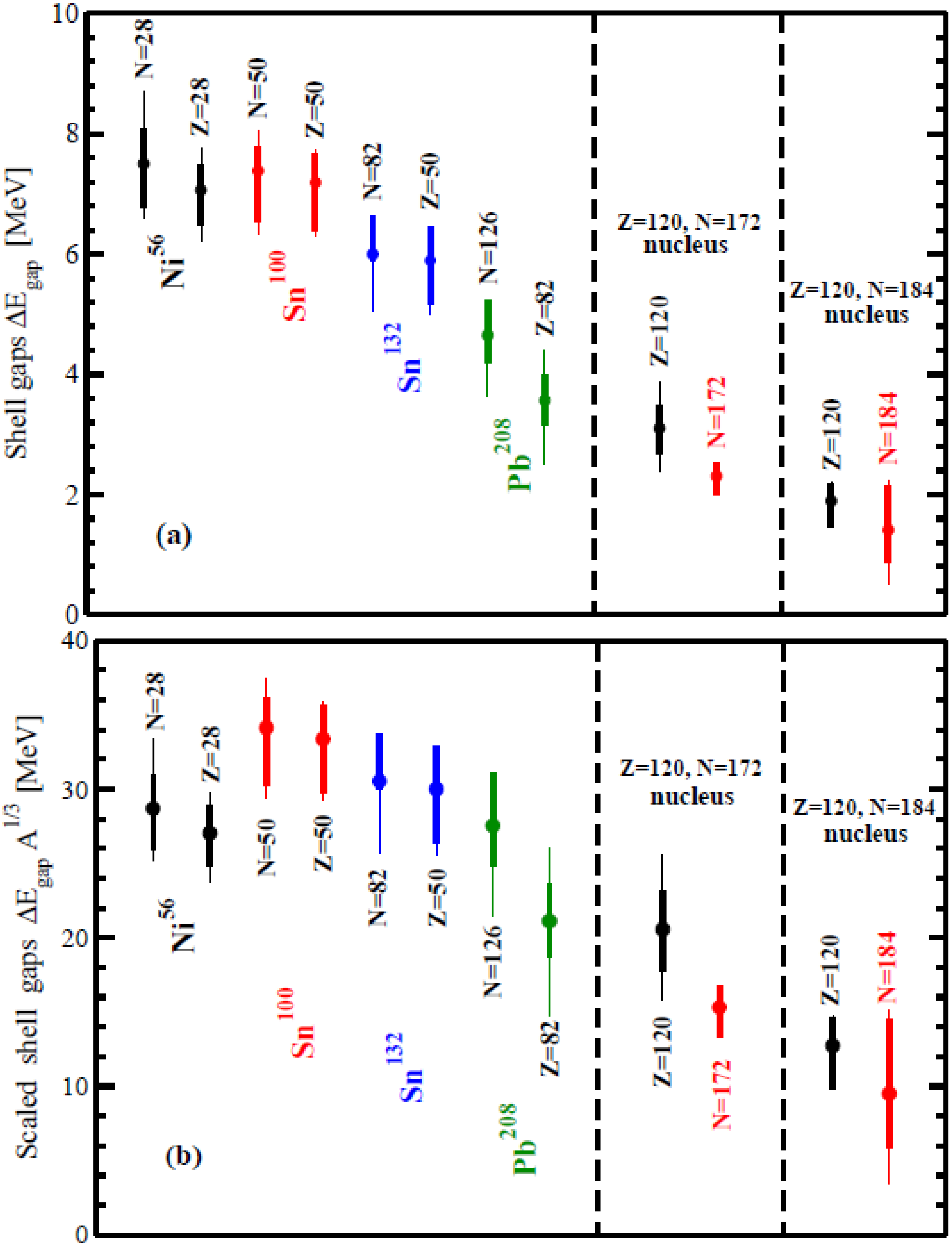

Thin lines – all 10 CEDF's, thick – 4 CEDF (NL3*,DD-ME2, DD-MEδ,DD-PC1)

Mass dependence of single-particle level density (~$A^{1/3}$) is taken into account

"Two-particle shell gaps": Hartree vs Hartree-Fock results

$$\delta_{2p}(N,Z) = S_{2p}(N,Z) - S_{2p}(N,Z+2),$$

$$\delta_{2n}(N,Z) = S_{2n}(N,Z) - S_{2n}(N+2,Z).$$

Li *et al*, PLB 732, 169 (2014)

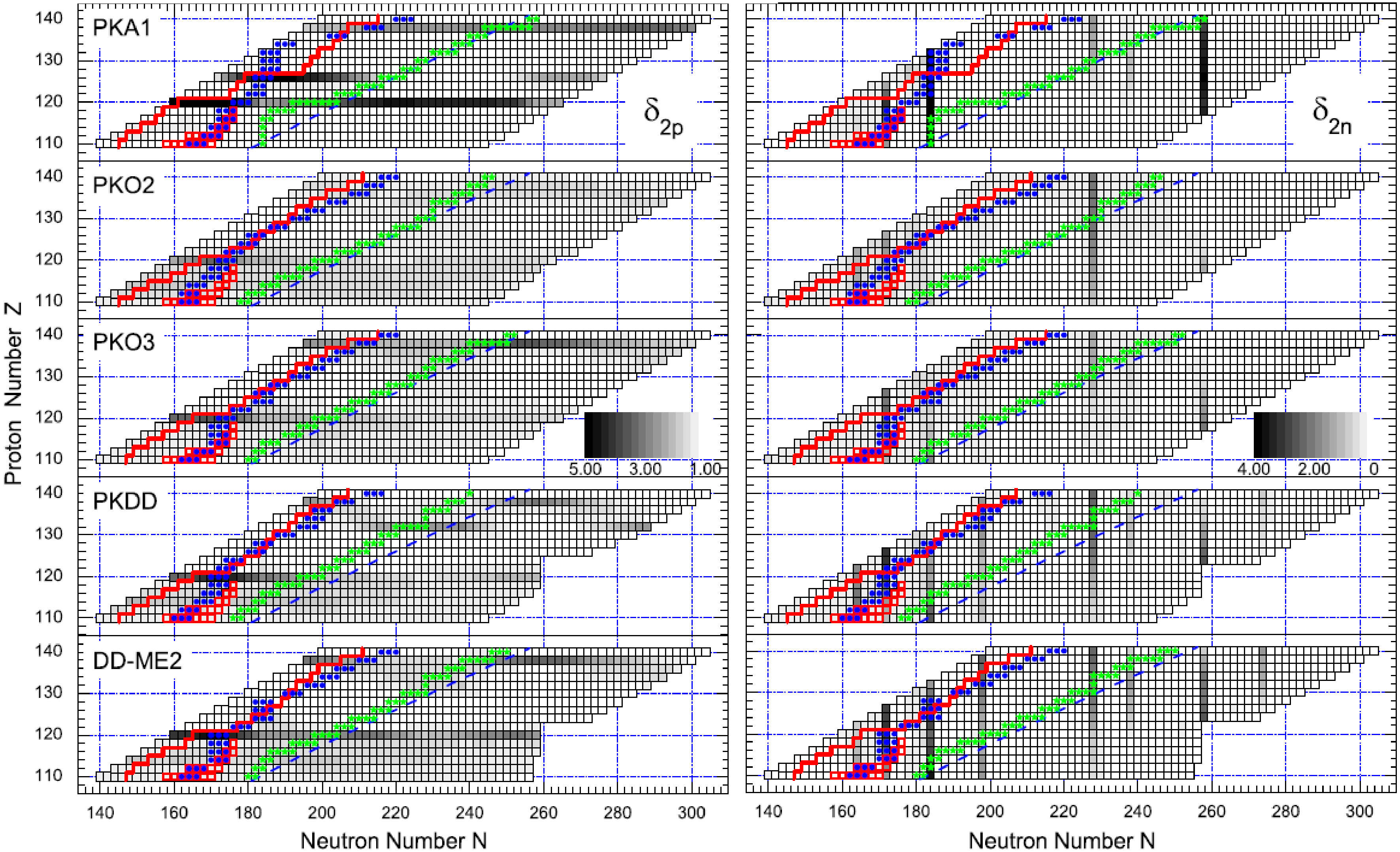

"Two-particle shell gaps": misleading quantity?

$$\delta_{2p}(N,Z) = S_{2p}(N,Z) - S_{2p}(N,Z+2),$$
$$\delta_{2n}(N,Z) = S_{2n}(N,Z) - S_{2n}(N+2,Z).$$

M. Bender et al, PRC 58 (1998) 2126.
W. Zhang et al, NPA 753, 106 (2005).
Li *et al*, PLB 732, 169 (2014)

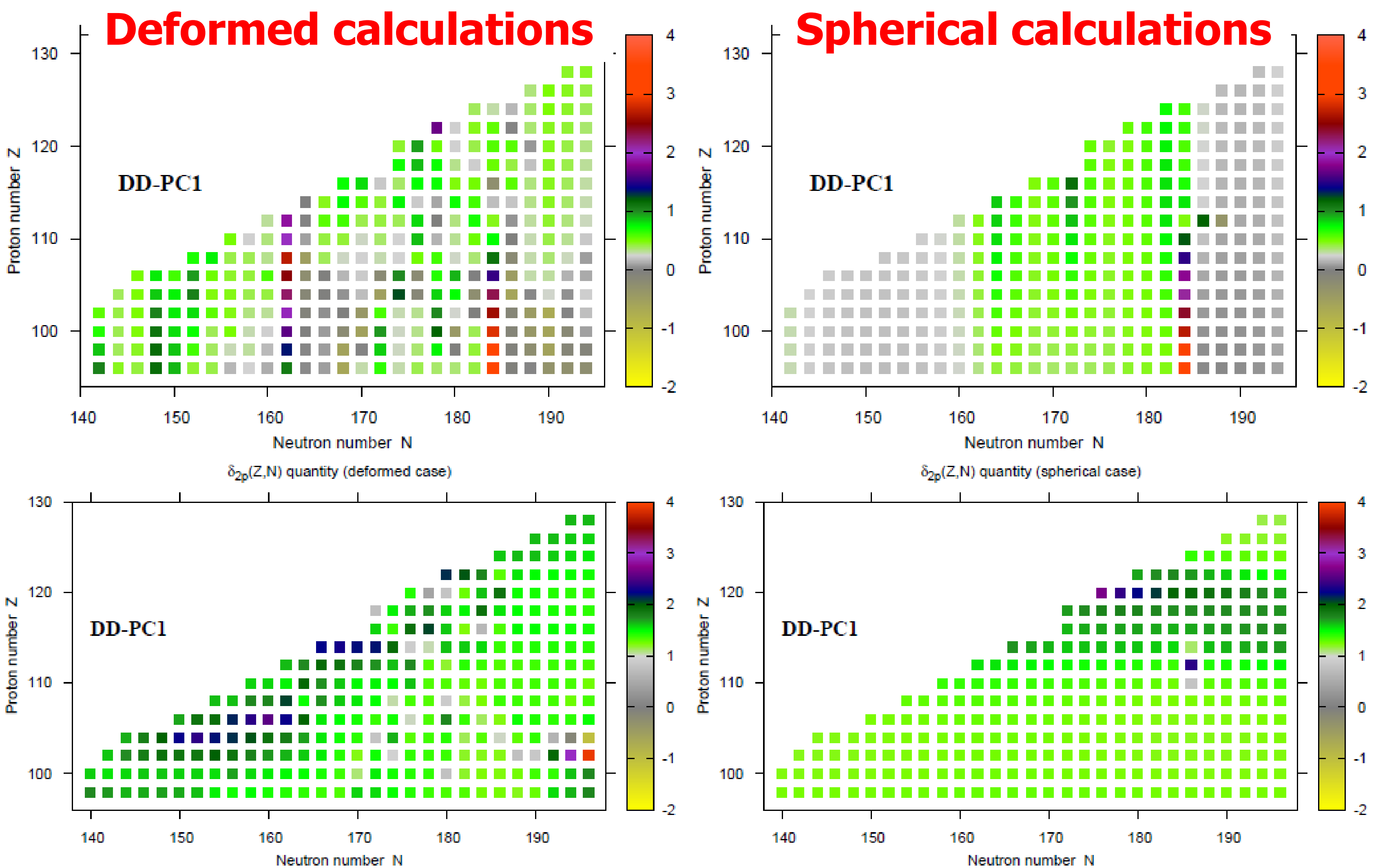

Deformation effects on shell structure

→ Very important – deformed results differ substantially from spherical ones

Unusual feature: oblate shapes above the shell closures

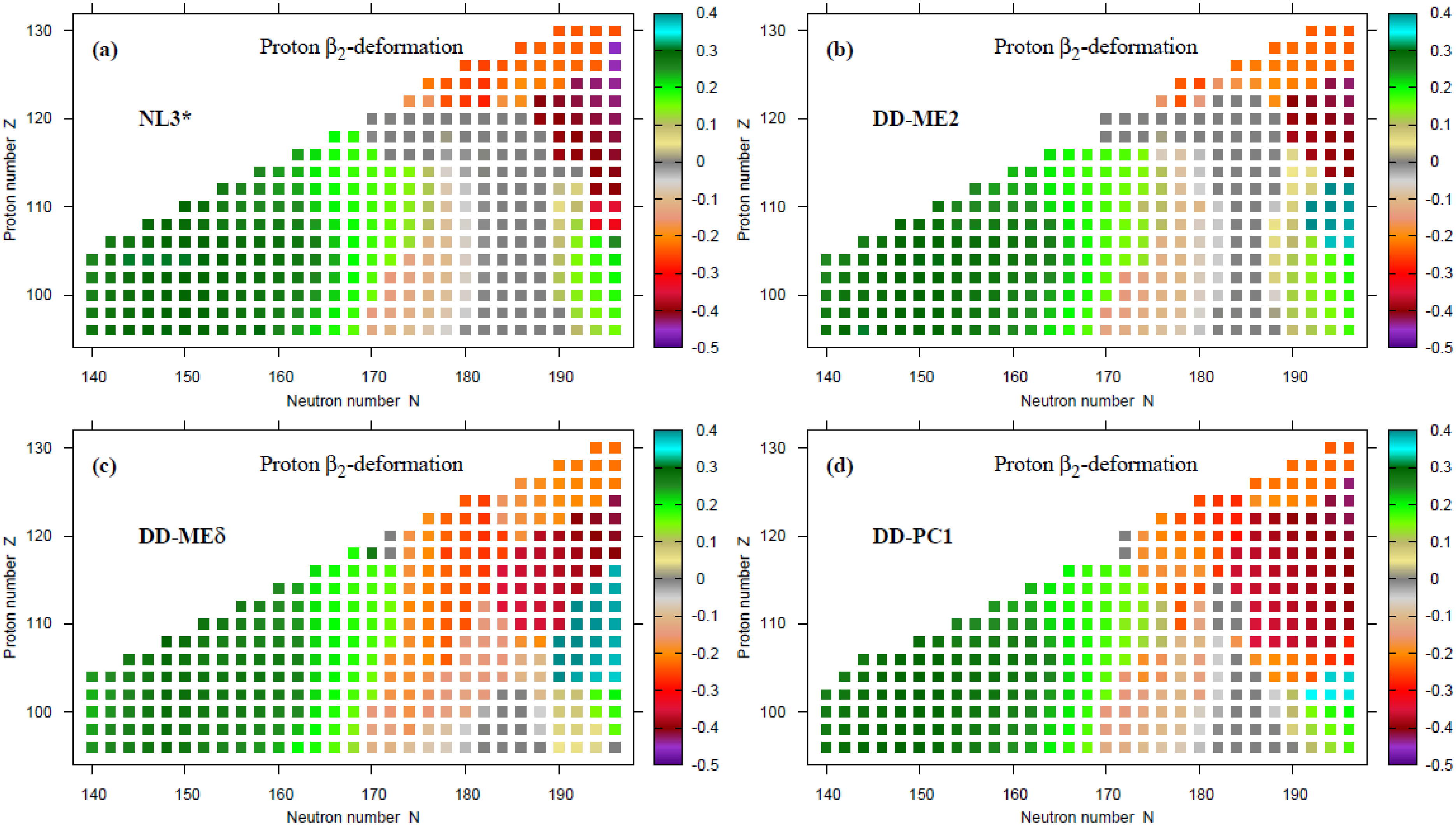

Results for PC-PK1 are very similar to the ones with NL3*

Shell correction energy: difference between tin and SHE regions

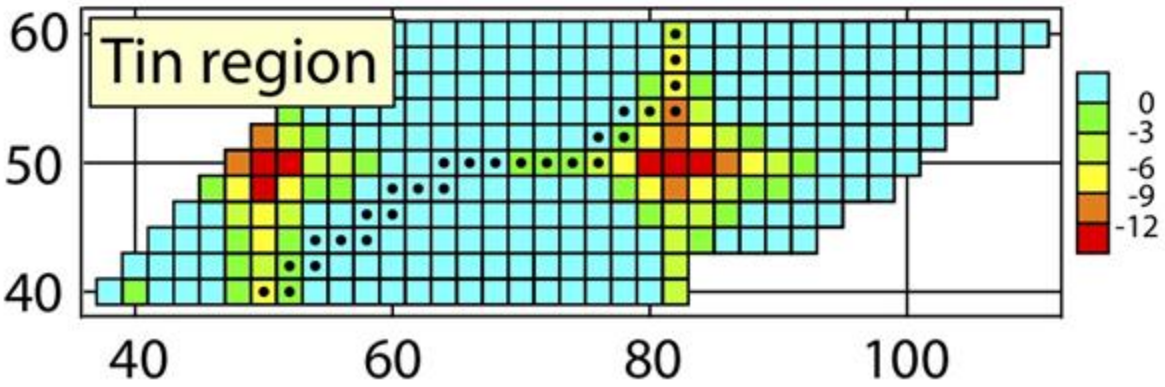

M.Bender, W.Nazarewicz, P.-G.Reinhard, PLB 515, 42 (2001)

Spherical calculations

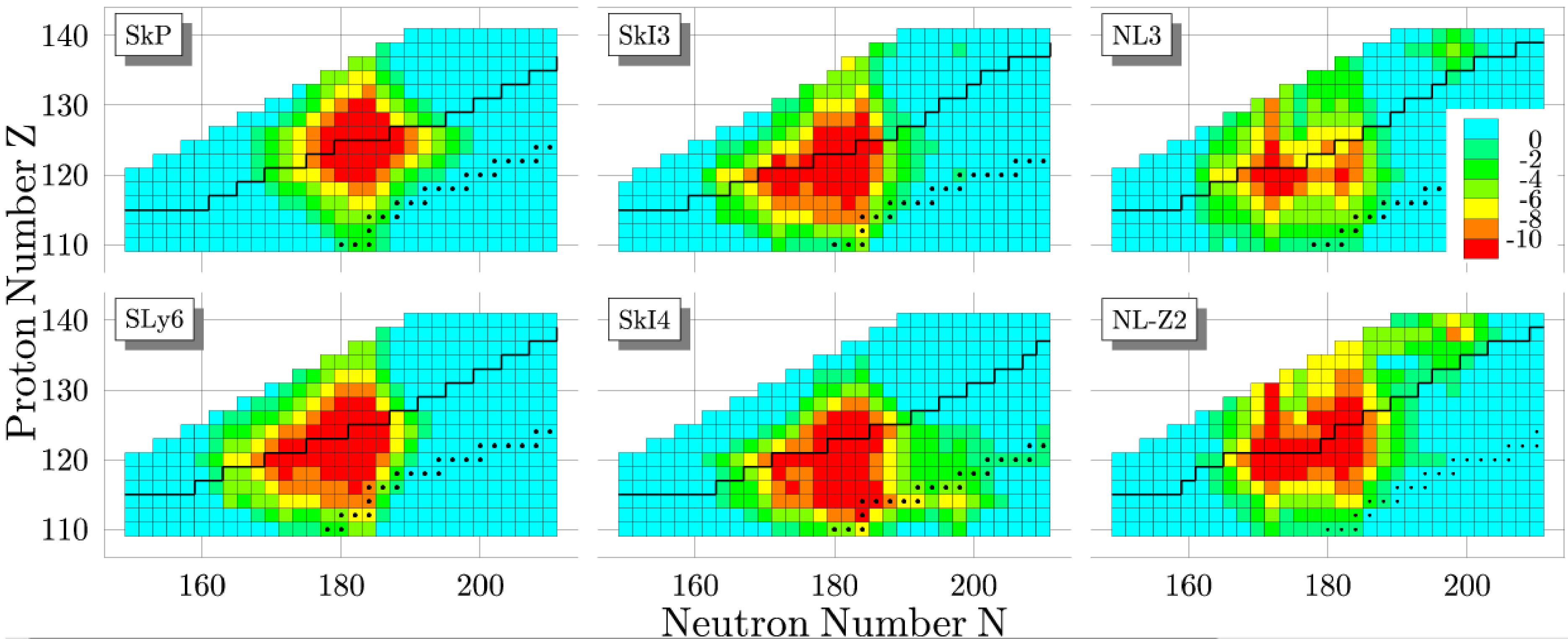

The spreads (theoretical uncertainties) in the deformations

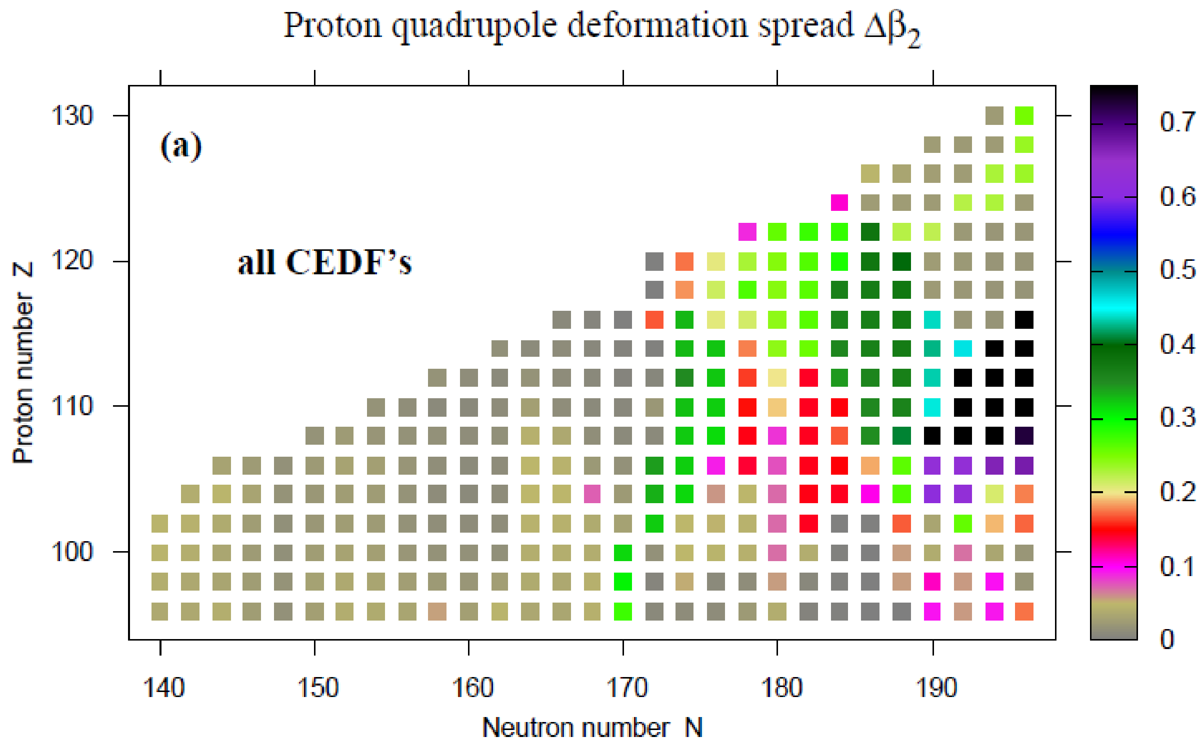

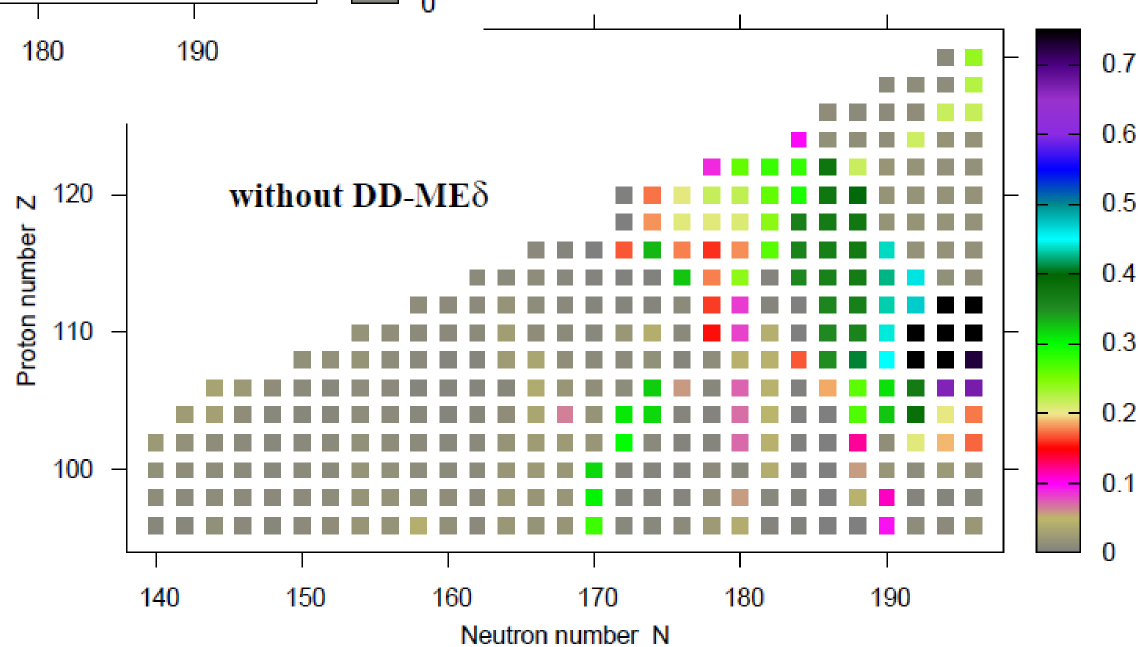

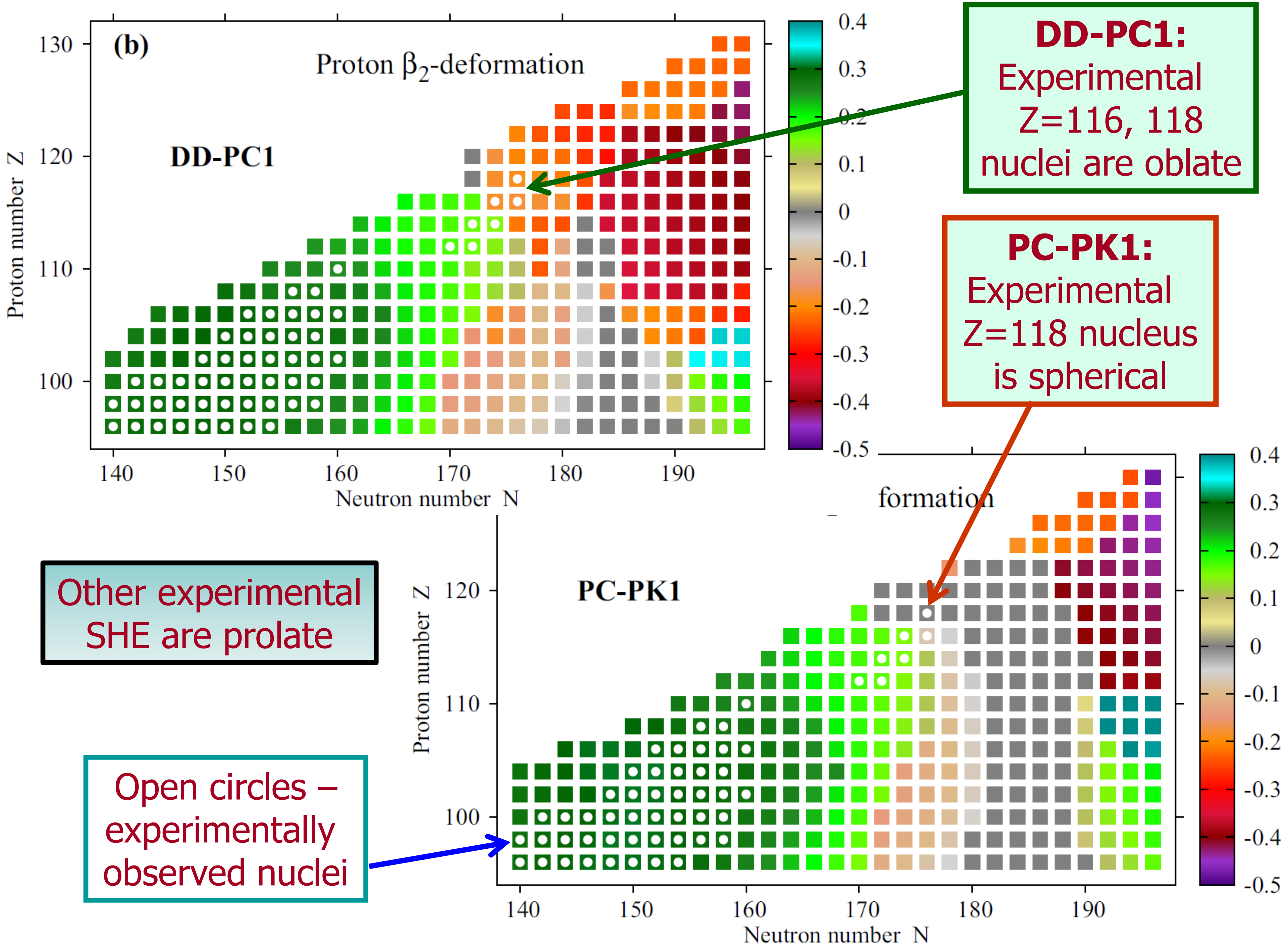
(b)
Proton β2-deformation
DD-PC1
Proton number Z
Neutron number N
130
120
110
100
140
150
160
170
180
190
0.4
0.3
0.2
0.1
0
-0.1
-0.2
-0.3
-0.4
-0.5
DD-PC1:
Experimental
Z=116, 118
nuclei are oblate
PC-PK1:
Experimental
Z=118 nucleus
is spherical
formation
PC-PK1
Other experimental
SHE are prolate
Open circles –
experimentally
observed nuclei

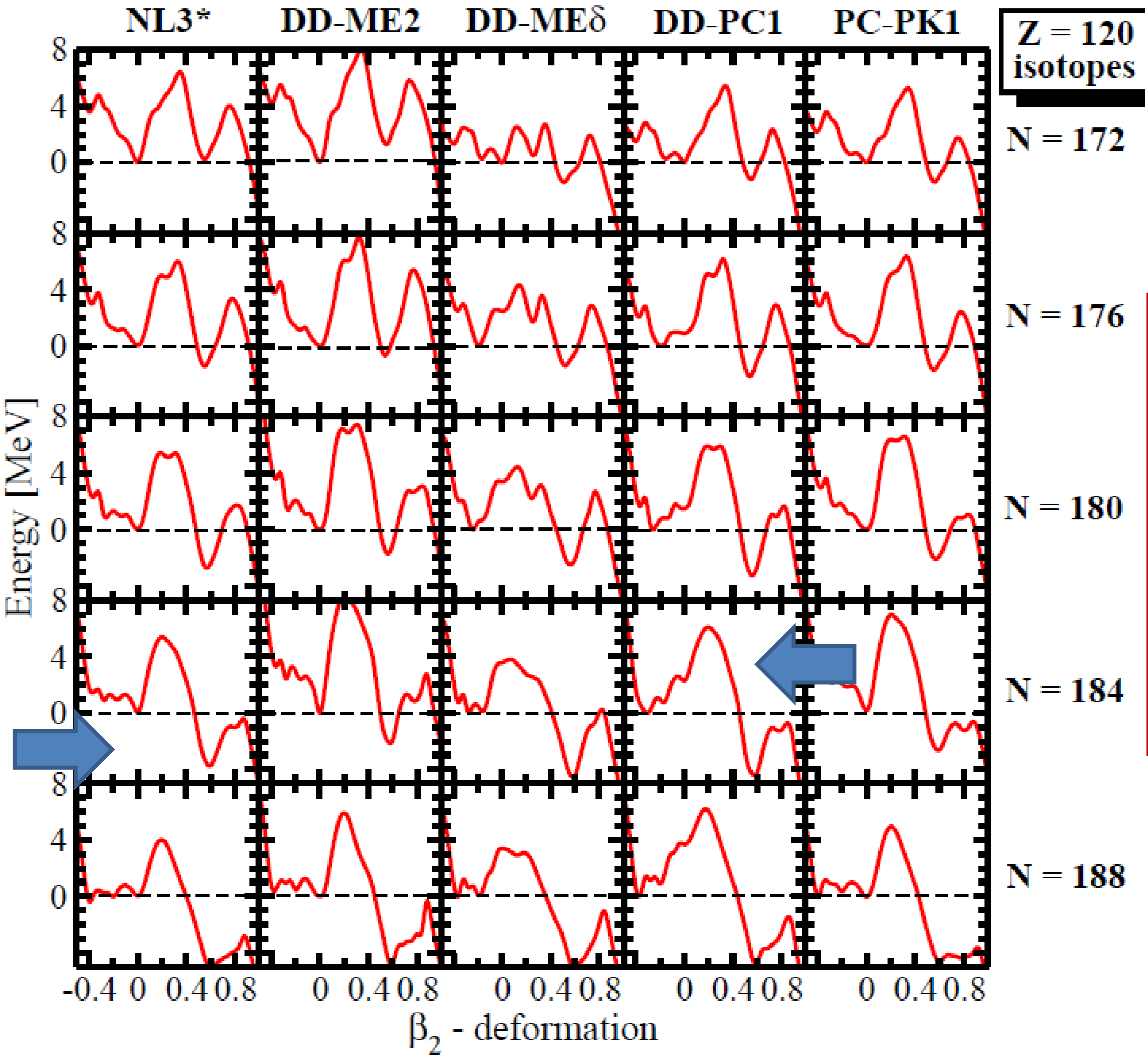

Potential energy surfaces in axially symmetric RHB calculations with separable pairing

The source of oblate shapes – the low density of s-p states

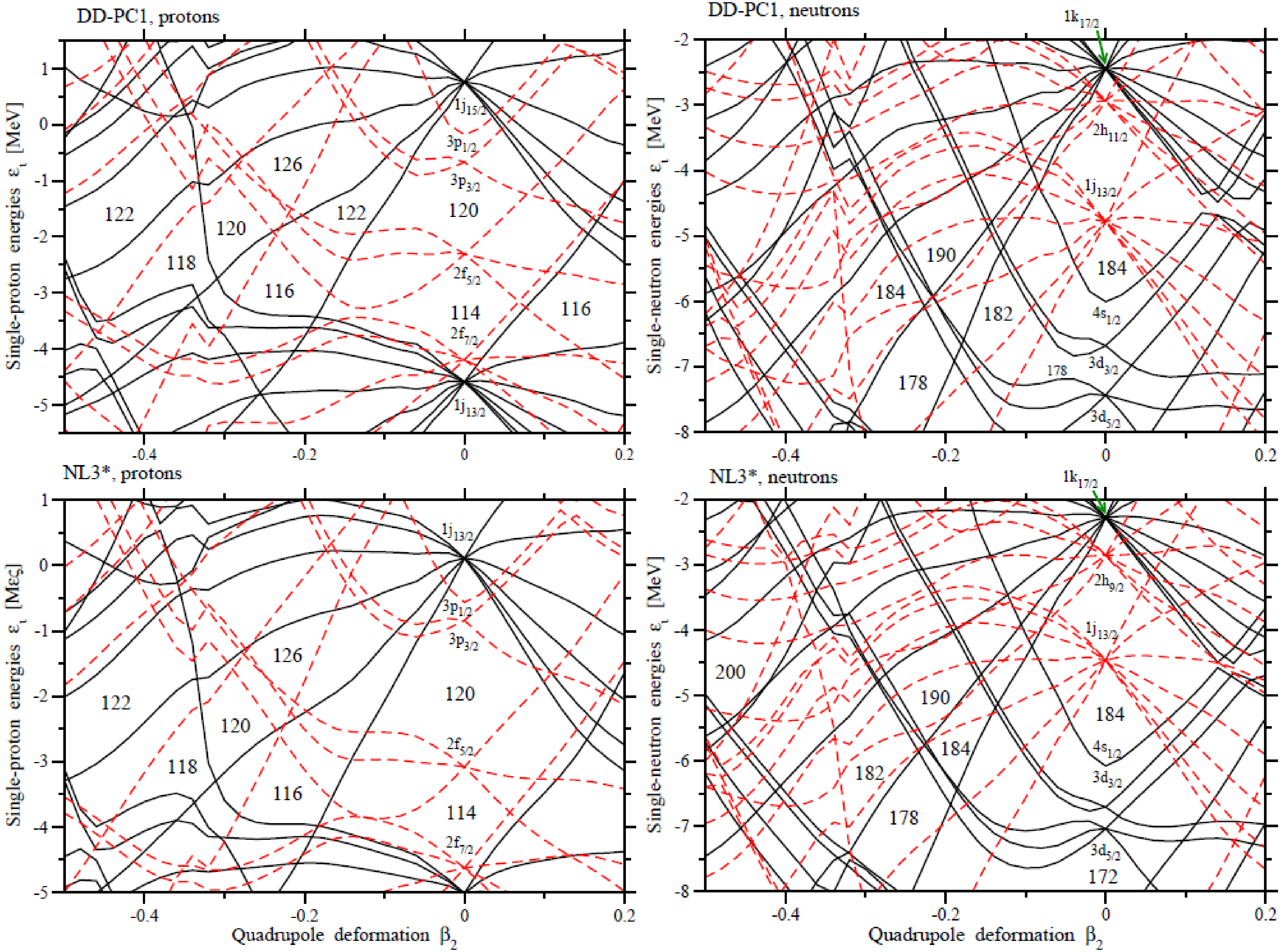

Accuracy of the description of experimental data in Z>94 nuclei

CEDF	ΔE_{rms} [MeV]	$\Delta(S_{2n})_{rms}$ [MeV]	$\Delta(S_{2p})_{rms}$ [MeV]	$\Delta(Q_{\alpha})_{rms}$ [MeV]
1	2	3	4	5
NL3*	3.02/3.39	0.71/0.68	1.33/1.34	0.68/0.75
DD-ME2	1.39/1.40	0.45/0.54	0.85/0.90	0.51/0.65
DD-MEδ	2.52/2.45	0.60/0.51	0.45/0.48	0.39/0.51
DD-PC1	**0.59/0.74**	0.30/0.32	0.41/0.42	0.36/0.47
PC-PK1	2.82/2.63	**0.25/0.23**	**0.36/0.33**	**0.32/0.38**

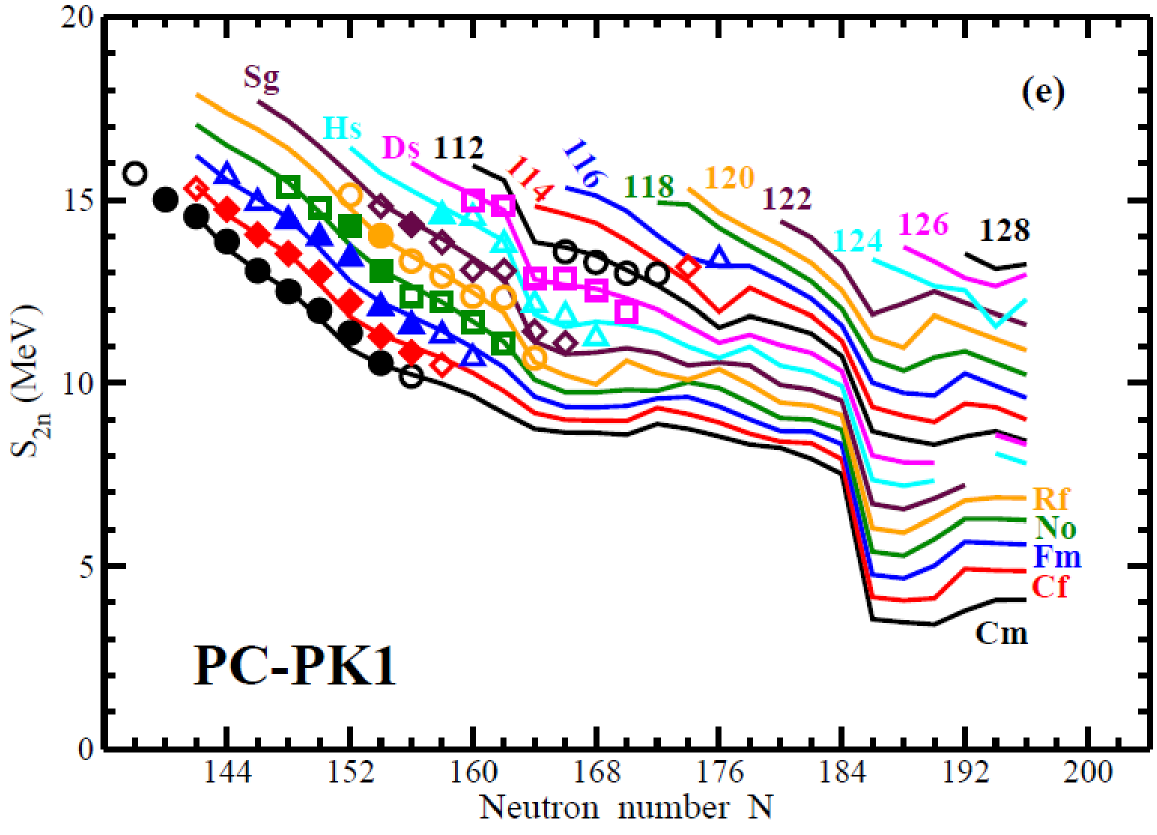

With exception of the DD-MEδ, the deformed N=162 gap is well reproduced in all CEDF's

The Q_α-values

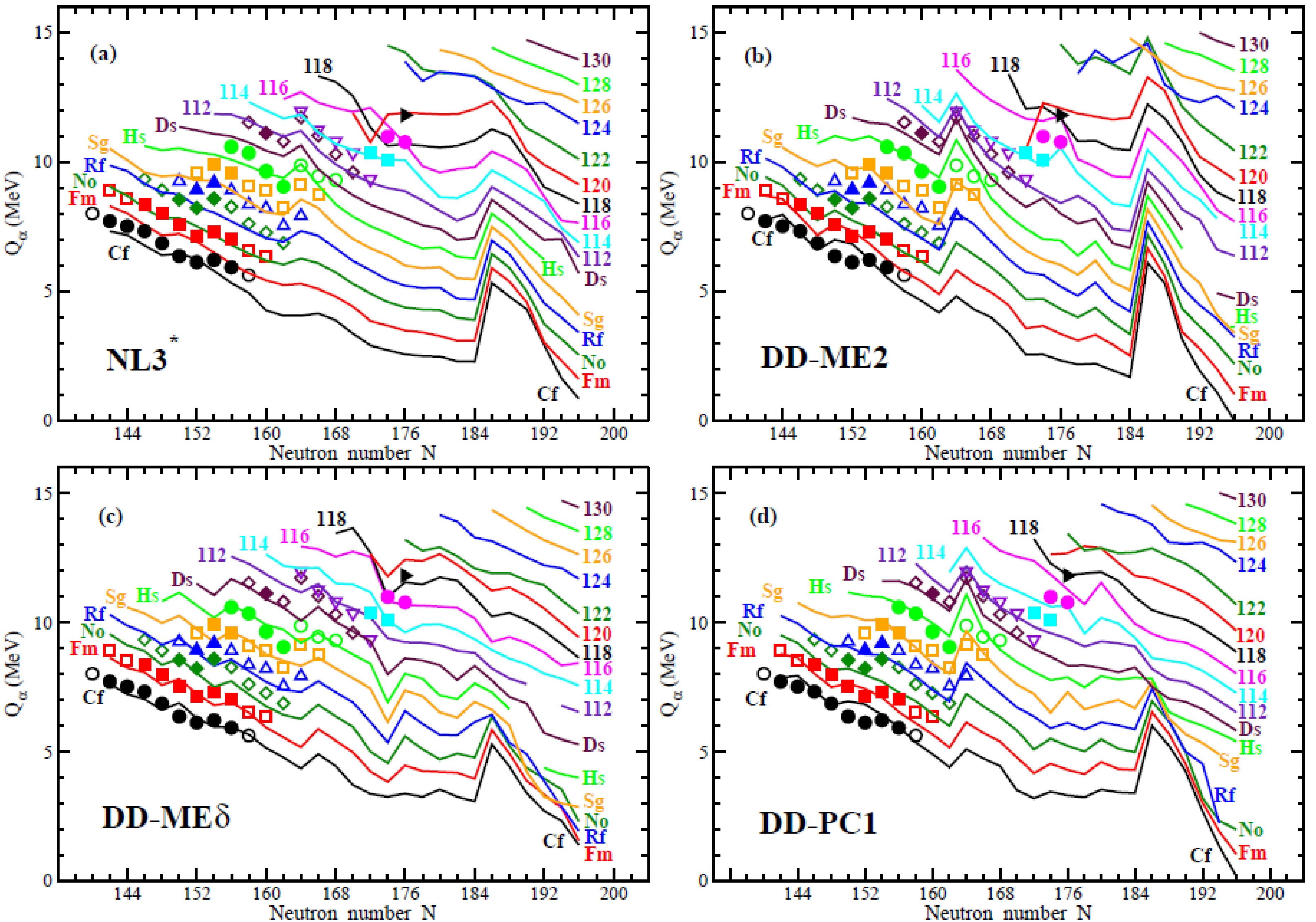

The heights of inner fission barriers in superheavy nuclei

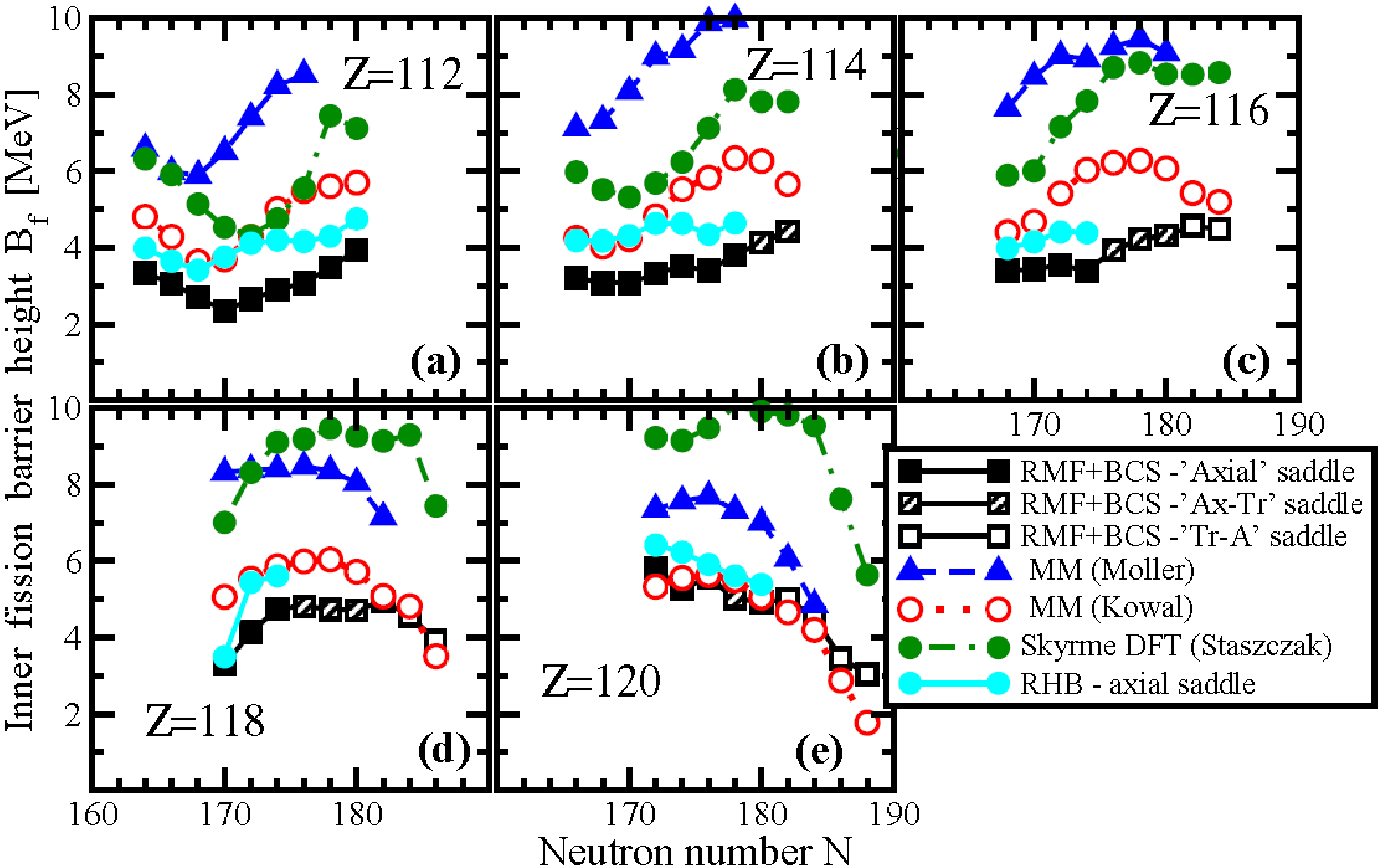

AA, S. Agbemava, Acta Physica Polonica, 46, 405 (2015)

A. Staszczak et al, PRC 87, 024320 (2013) – Skyrme SkM*
M. Kowal et al, PRC 82, 014303 (2010) – WS pot. + Yukawa exponent. model
P. Moller et al, PRC 79, 064304 (2009) – folded Yukawa pot. + FRDM model

Inner fission barrier heights with different covariant density functionals: according to axial RHB calculations

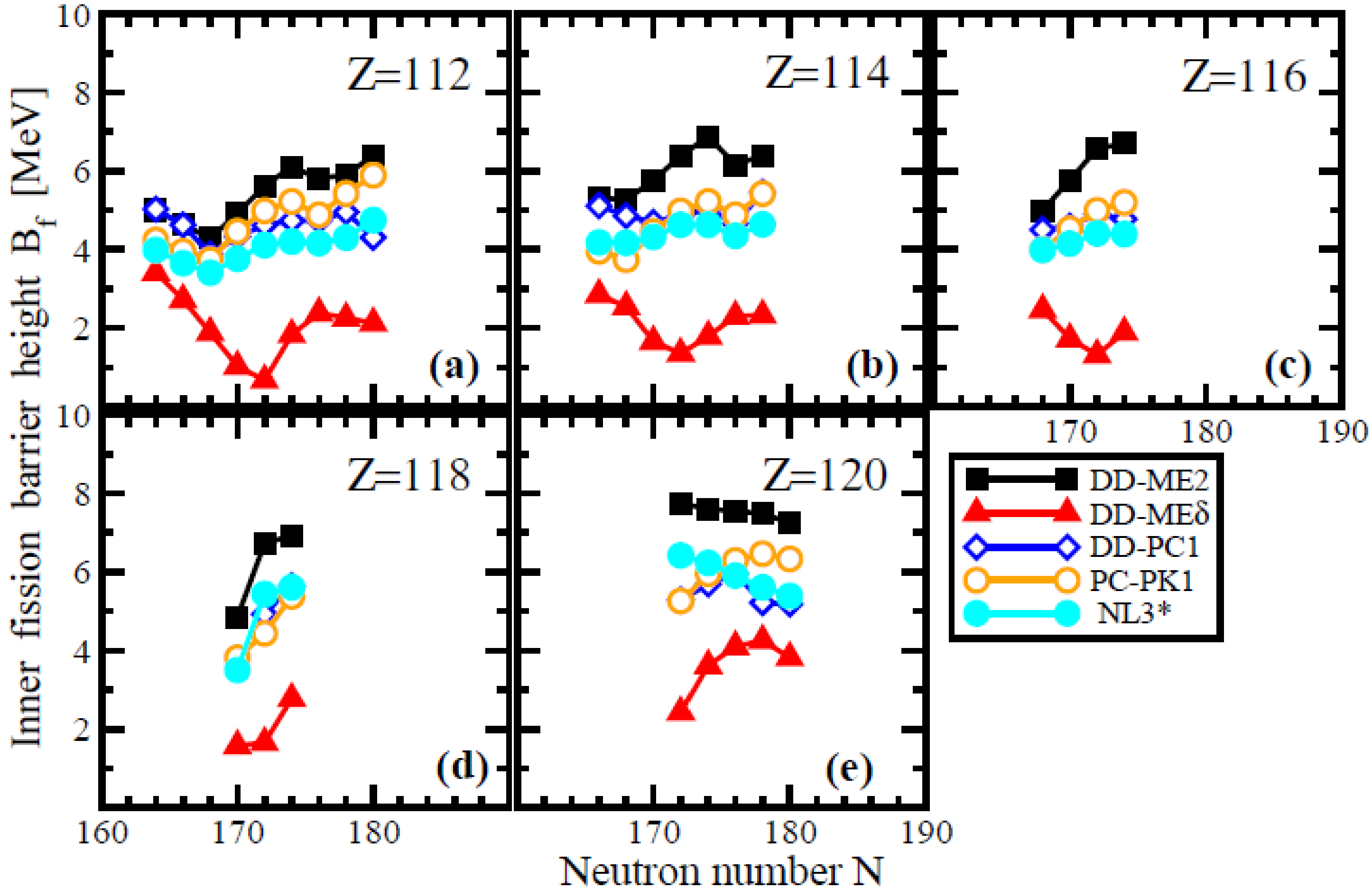

The results are shown only for nuclei which have axial saddles in the triaxial RMF+BCS calculations with the NL3* functional

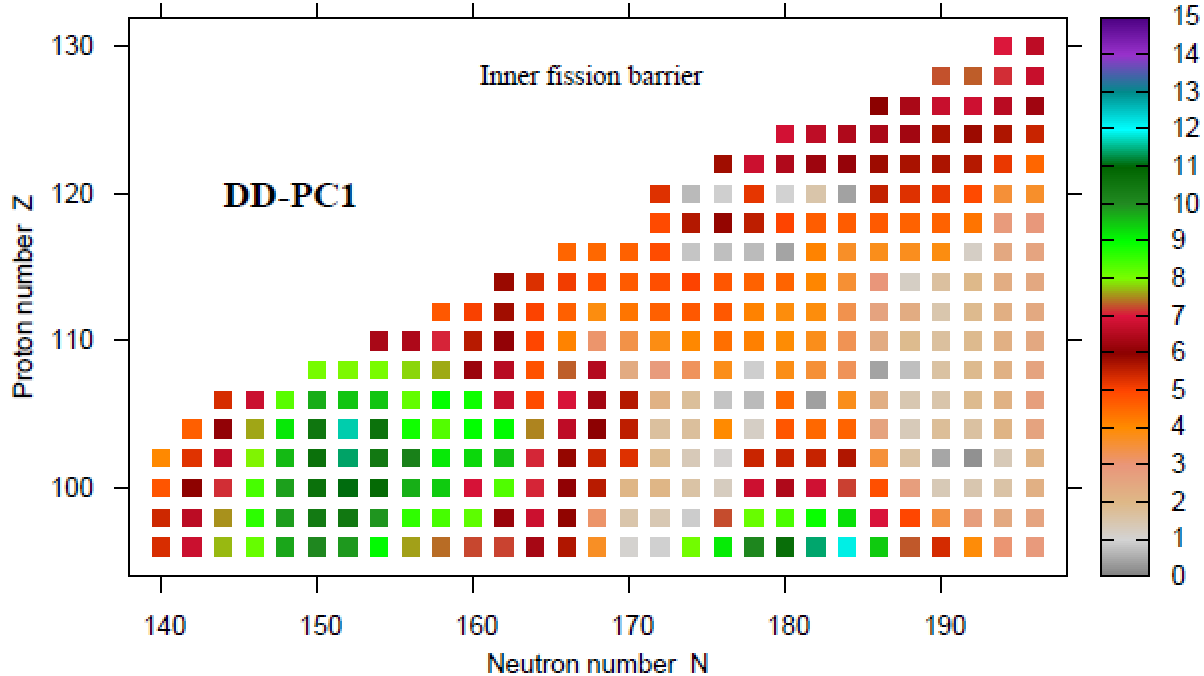

Inner fission barrier heights as obtained in axially symmetric RHB with separable pairing

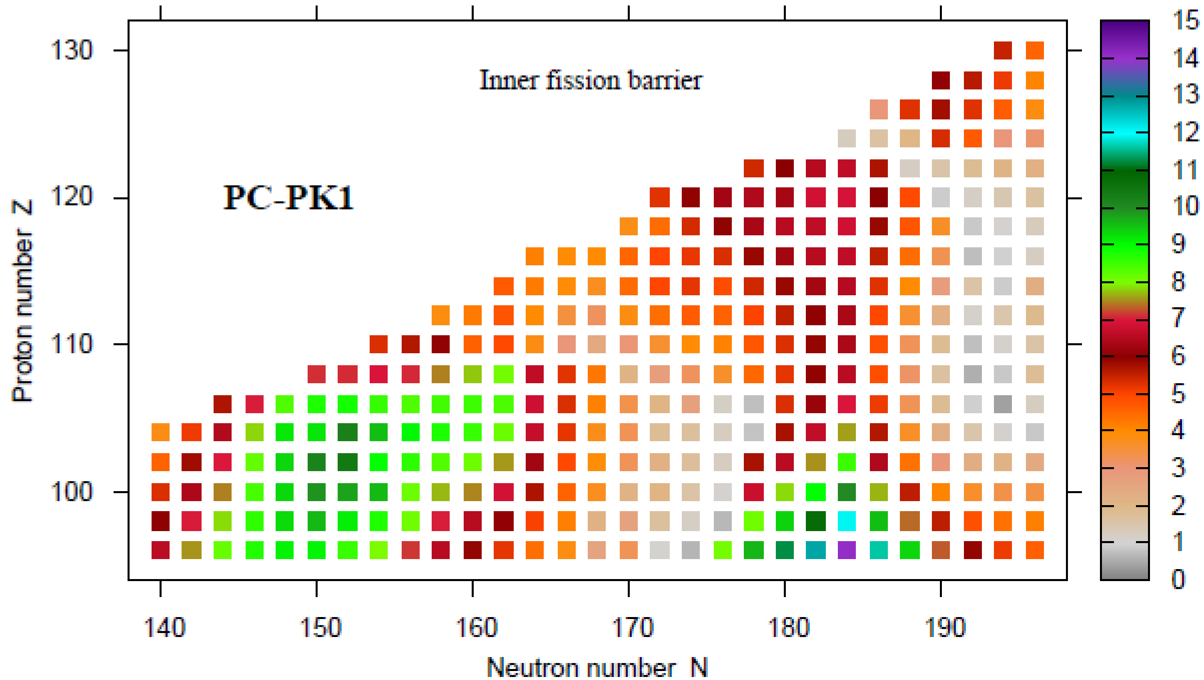

provides upper limit for inner barrier height

The spreads (theoretical uncertainties) in the heights of inner fission barriers in superheavy nuclei

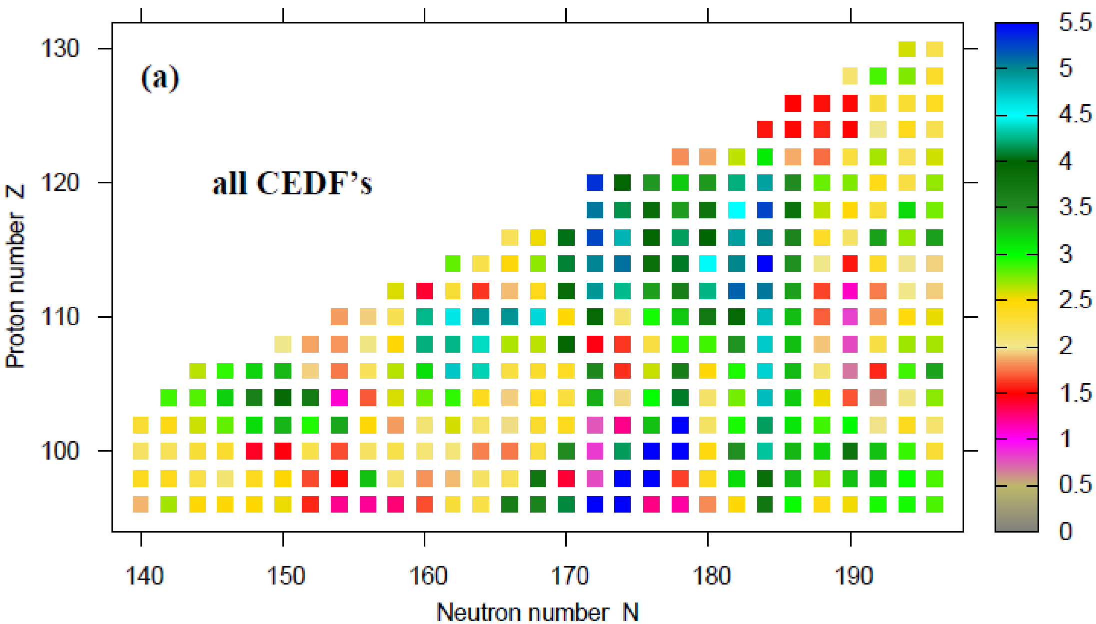

Benchmarking of fission barriers in actinides (done for NL3*, DD-PC1 and PC-PK1) reduces theoretical uncertainties and makes the description of fission barriers more predictive

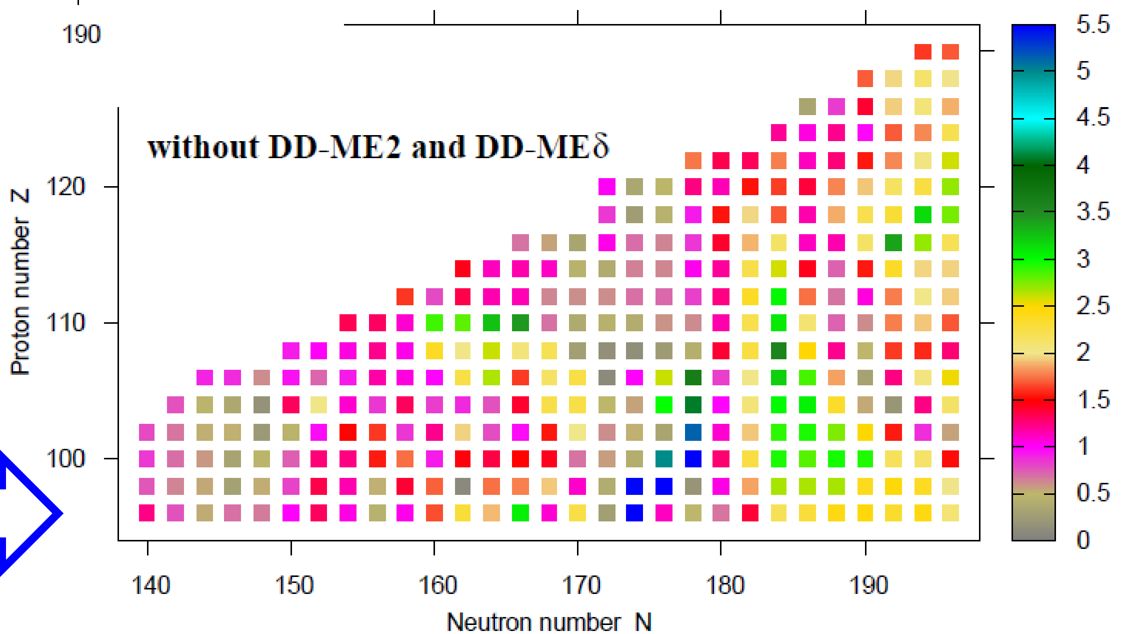

Fission recycling in dynamically ejected matter of neutron star mergers.

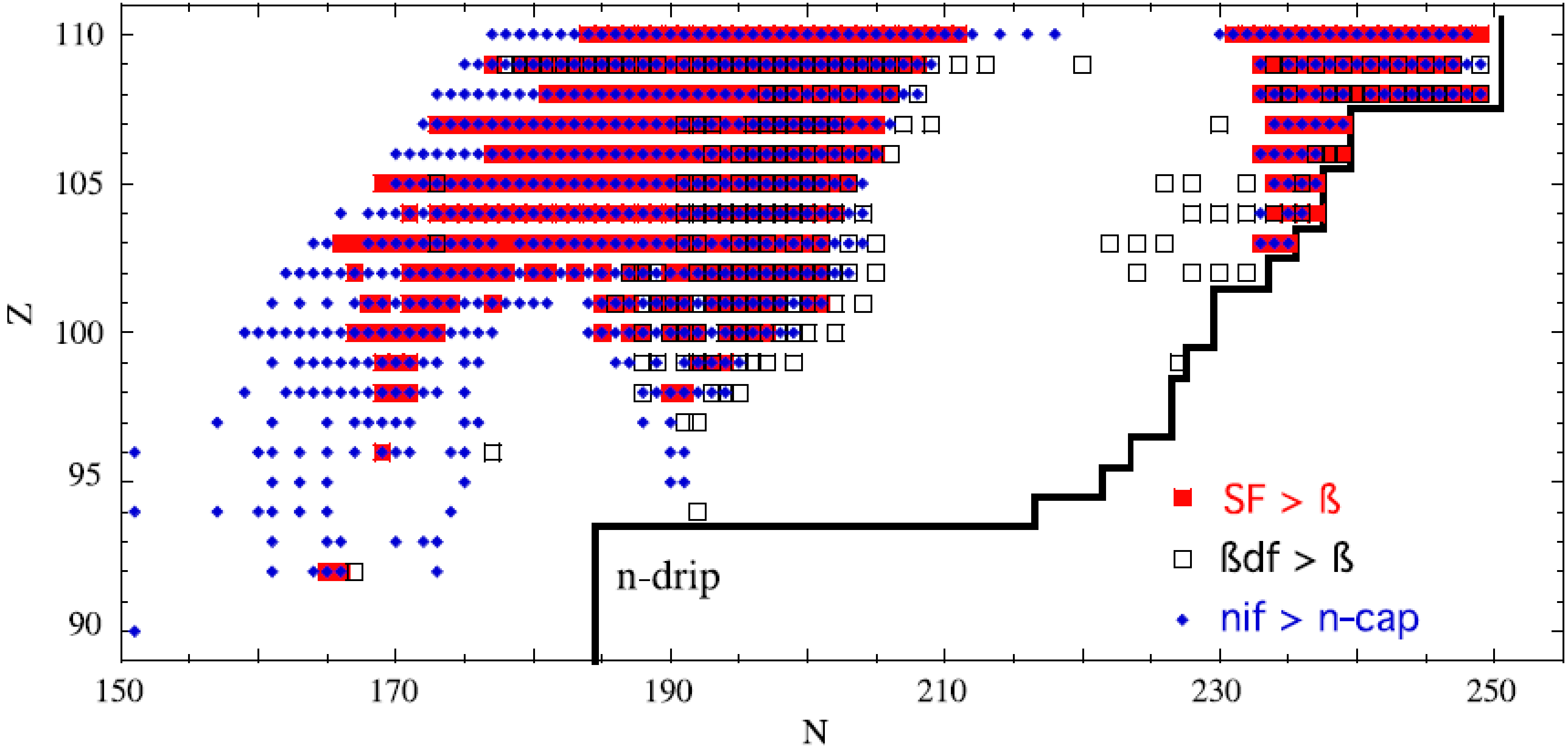

Dominant fission regions in the (N,Z) plane. Nuclei for which spontaneous fission is estimated to be faster than b-decays are shown by full squares, those for which β-delayed fission is faster than β-decays by open circles, and those for which neutron-induced fission is faster than radiative neutron capture at $T=10^9$ by diamonds.

From S. Goriely et al, AJL 738, L32 (2011)

Single-particle energies: how to improve their description?

Impact of quasiparticle-vibration coupling on the spectra

NL3* covariant energy density functional

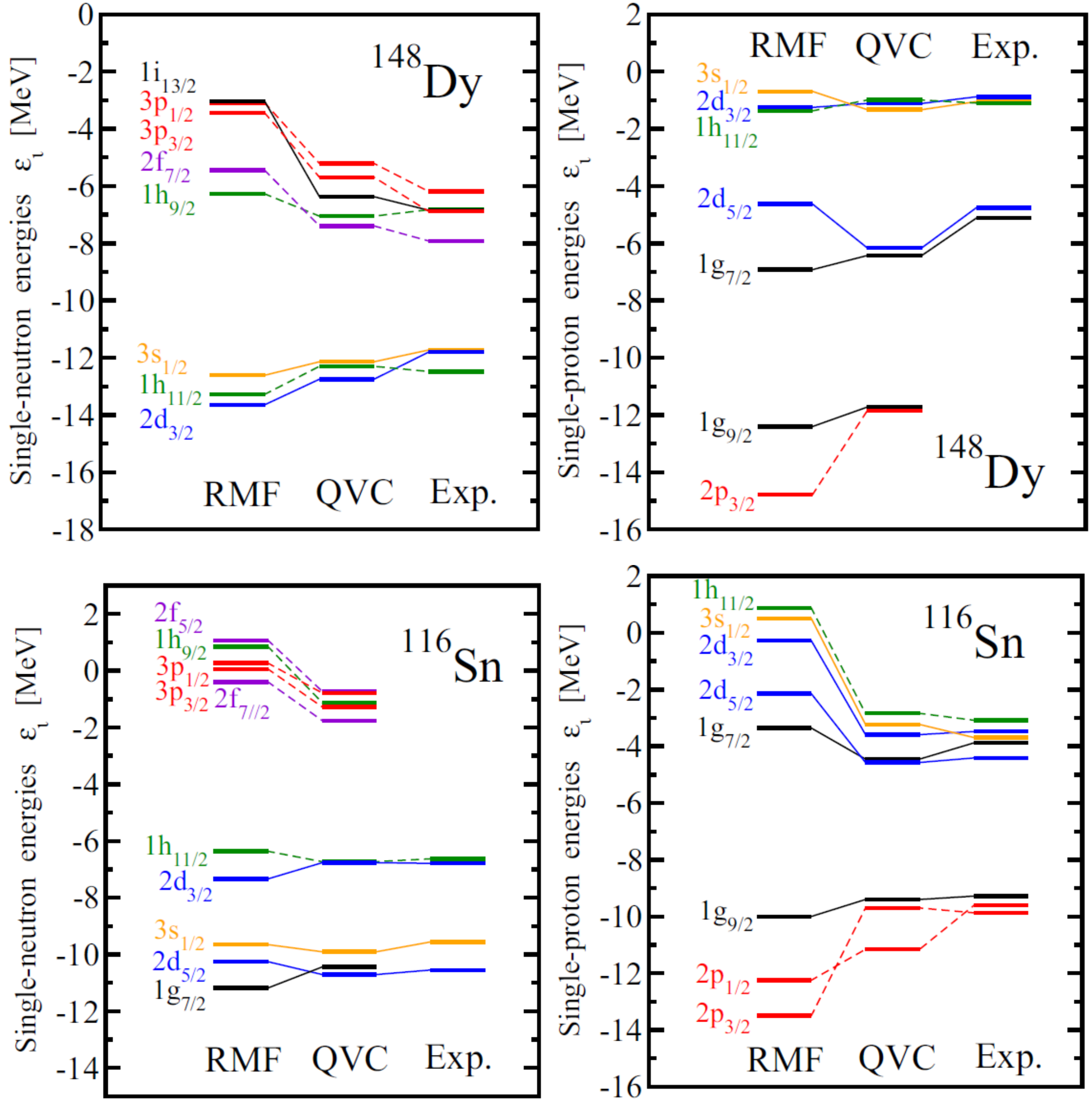

AA, E.Litvinova, PRC 92, 044317 (2015)

Tensor interaction in Skyrme DFT

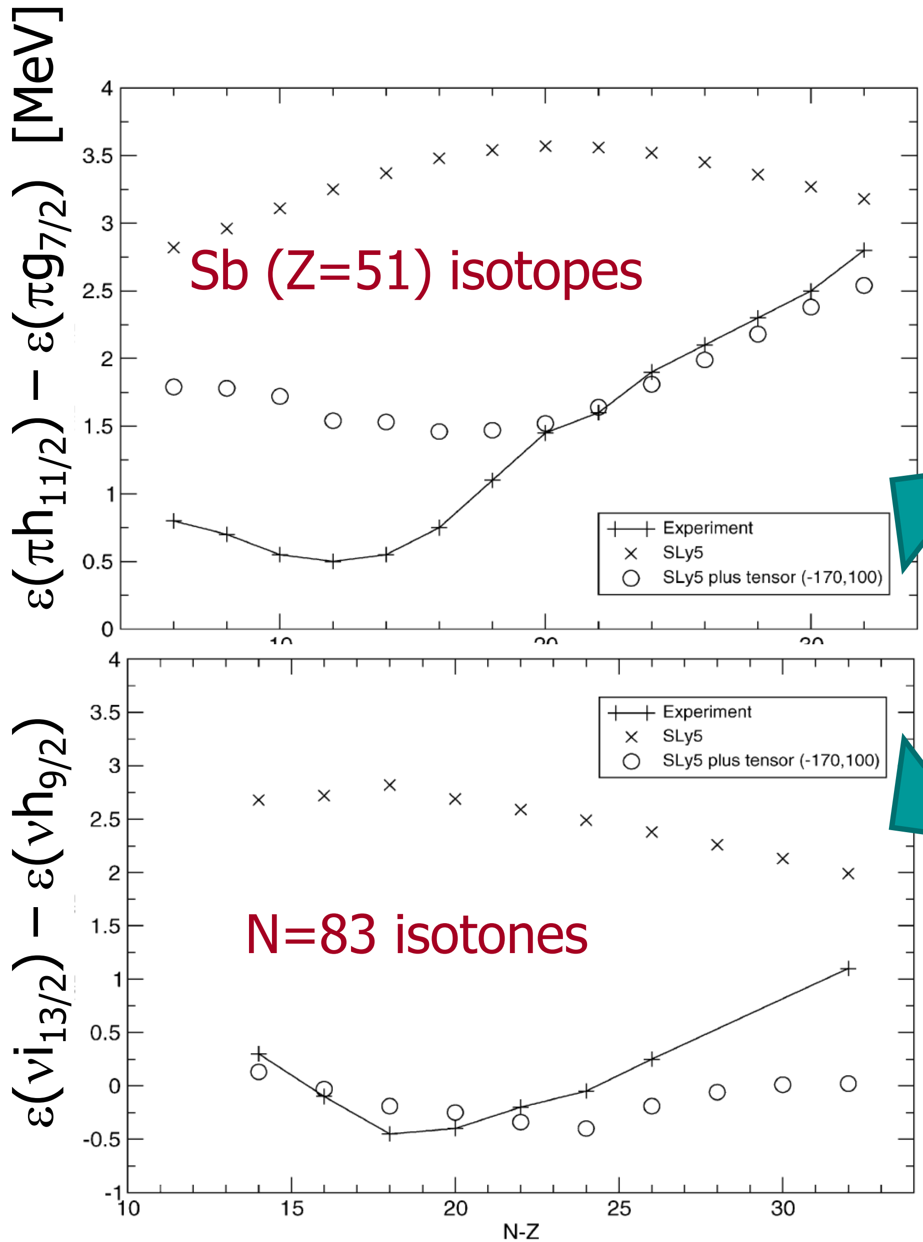

Recent extensive review on effective tensor interaction – H.Sagawa and G. Colo, PPNP 76, 76 (2014).

Strongest "evidence" for effective tensor interaction from the energy splitting of spherical states

Skyrme DFT - G. Colo et al, PLB 646 (2007) 227

Other examples: CDFT and Gogny DFT

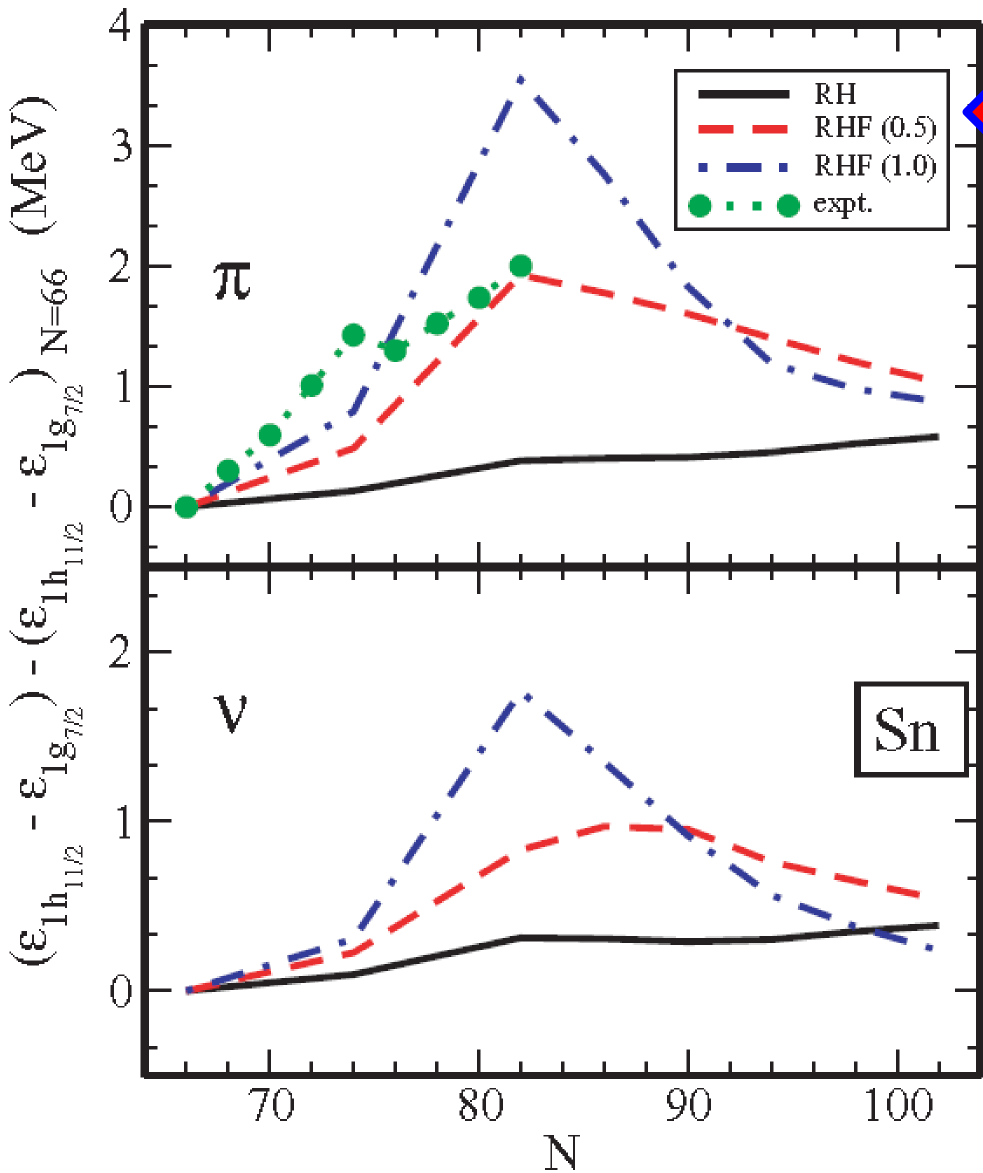

Relativistic Hartree-Fock - pion tensor coupling
G. A. Lalazissis et al, PRC 80, 041301 (2009)

Gogny D1S
GT2 = D1S + plus tensor force
- T. Otsuka et al, PRL 97, 162501 (2006)

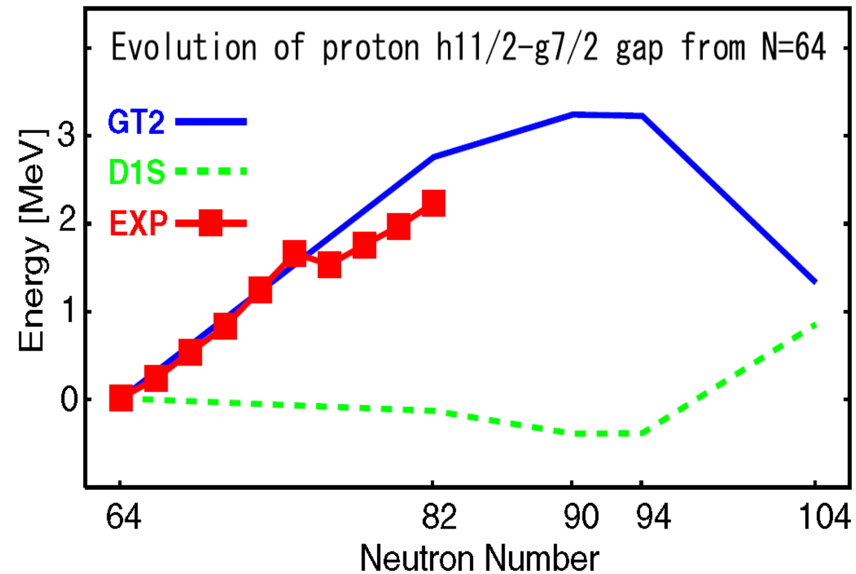

Relativistic quasiparticle-vibration coupling calculations: **(1)** the NL3* functional and **(2)** no tensor interaction

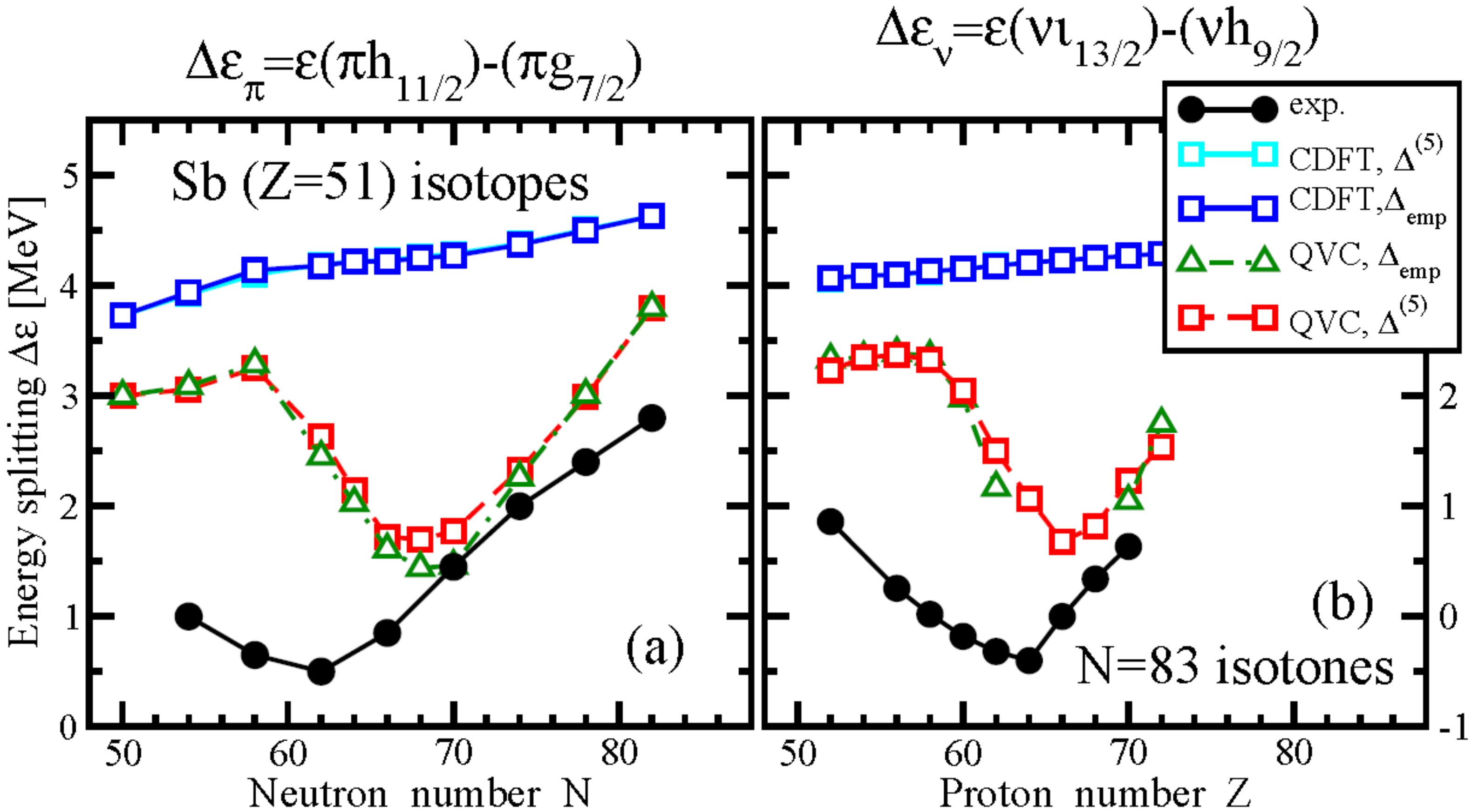

Our analysis clearly indicates that both QVC and tensor interaction act in the same direction and reduce the discrepancies between theory and experiment for the splittings of interest. As a consequence of this competition, the effective tensor force has to be weaker as compared with earlier estimates.

Fragmentation of the single-particle strength

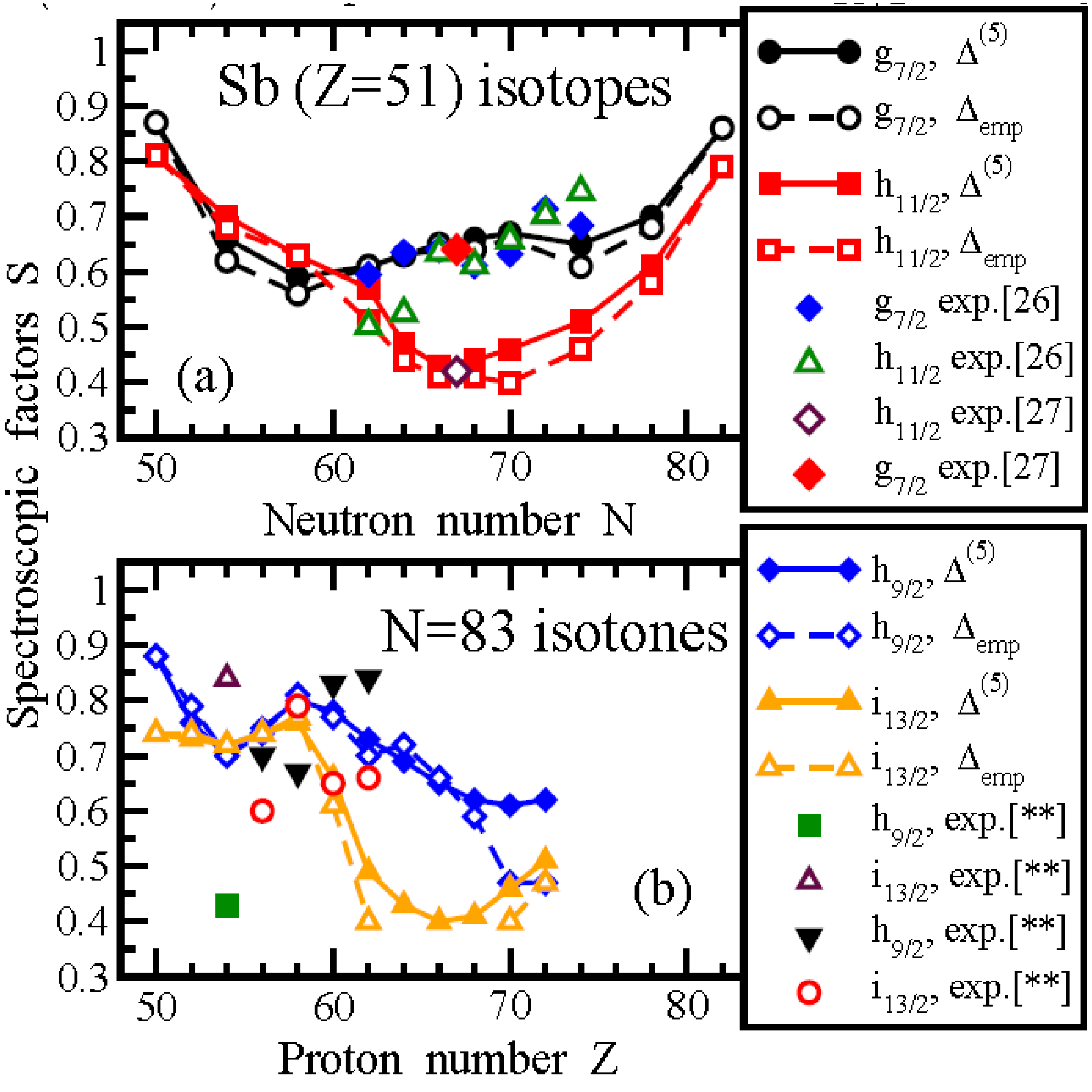

J. P. Schiffer et al, PRL 92, 162501 (2004) – the states of interest are single-particle ones (S=1)

J. Mitchell, PhD thesis, University of Manchester, (2012) – strong fragmentation of the single-particle strength (cannot be accounted at the DFT level)

M. Conjeaud et al, NPA 117, 449 (1968) and O. Sorlin Prog. Part. Nucl. Phys. 61, 602 (2008) also support low S~0.5 for $\pi h_{11/2}$ state in mid-shell Sb isotopes

B.P.Kay et al, PRC 84, 024325 (2011)
PLB 658, 216 (2008)

QVC versus tensor force

1. Both quasiparticle-vibration coupling and tensor interaction act in the same direction and reduce the discrepancies between theory and experiment for the $\Delta\varepsilon_\pi$ and $\Delta\varepsilon_\nu$ splittings.

2. As a consequence of this competition, the effective tensor force has to be considerably weaker as compared with earlier estimates.

3. The definition of the strength of the tensor interaction by means of the fitting to the energies of the dominant single-quasiparticle states in odd-mass nuclei is flawed without accounting for the effects of quasiparticle-vibration coupling.

Example of generic problems of many functionals: Deformed shell gaps at N=152 and Z=100

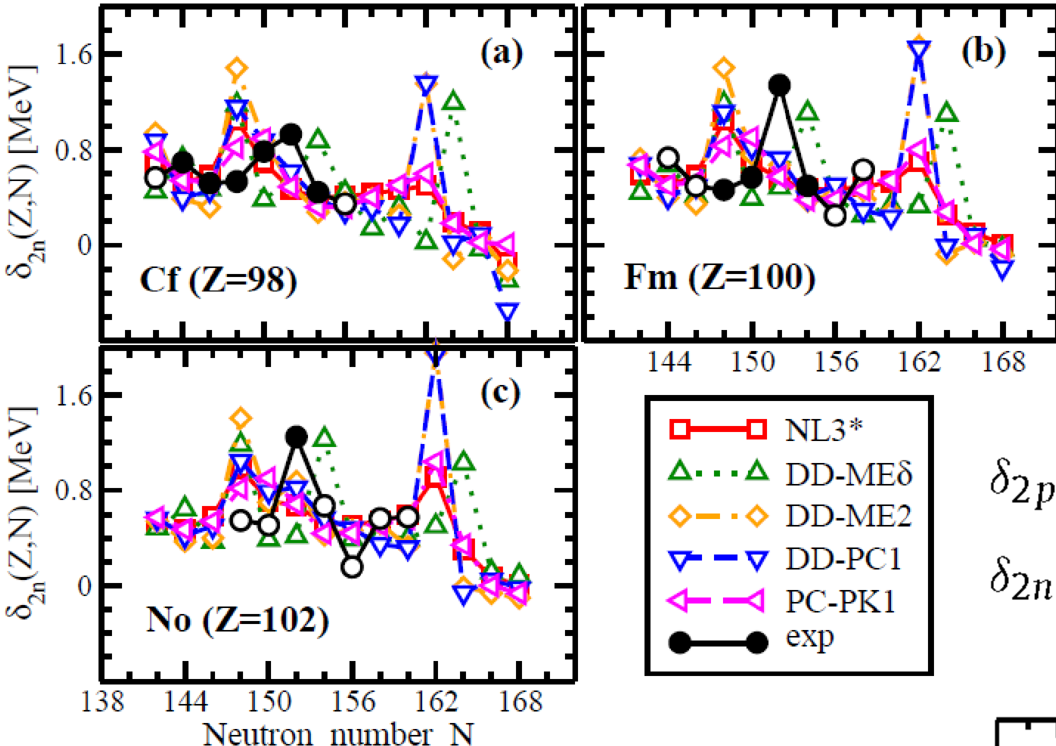

$$\delta_{2p}(N,Z) = S_{2p}(N,Z) - S_{2p}(N,Z+2),$$

$$\delta_{2n}(N,Z) = S_{2n}(N,Z) - S_{2n}(N+2,Z).$$

Towards spectroscopic quality DFT:

1. Improvement of the functionals at the DFT level

2. Accounting of (quasi)particle-vibration coupling

3. Inclusion of tensor interaction (not clear at this point)

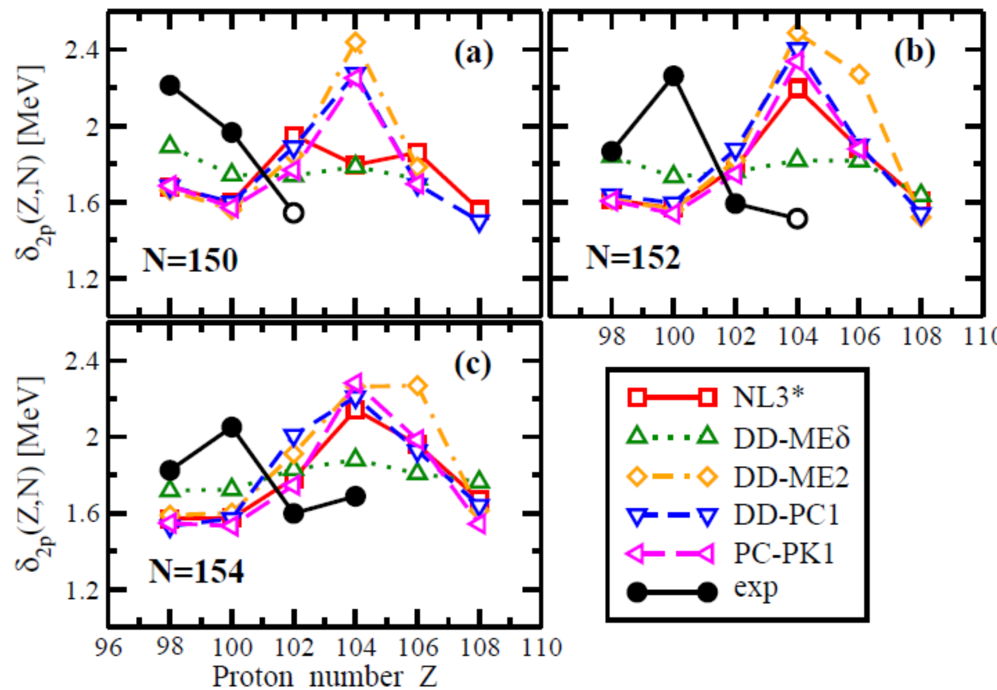

Thanks to my collaborators:

P.Ring (TU Munich)
S. Agbemava (MSU)
D.Ray (MSU)
T. Nakatsukasa (U. Tsukuba)
O. Abdurazakov (MSU)
J. Dobaczewski (U Warsaw)
L. Robledo (U Madrid)
Y. Shi (Michigan SU)
M. Bender

Conclusions

1. The impact of the N = 172 shell gap is very limited in the (Z,N) space for all functionals under investigation. The impact of the Z = 120 and N = 184 spherical shell gaps depend drastically on the functional. It is most pronounced for NL3* and PC-PK1 and is (almost) completely absent for DD-PC1 and DD-MEδ.

2. The accuracy of the description of known actinides and SHE and related theoretical uncertainties are quantified for a number of physical observables.

3. Available experimental data in SHE does not allow to give a clear preference to a specific functional predictions.

4. Be careful with the $\delta_{2n}(Z,N)$ and $\delta_{2p}(Z,N)$ predictions based on spherical calculations. Deformation effects are important even in close vicinity of expected shell gaps.